Preprints.org

Article

Not peer-reviewed version

Mathematical Modeling for the Optimal Surface of T-Shaped Combined Footing

Assuming That the Contact Area with the Ground Woks Partially Under Compression

Eyran Roberto Diaz-Gurrola , Arnulfo LUEVANOS ROJAS * , Griselda Santiago-Hurtado , Victor Manuel Moreno-Landeros , Aldo Emelio Landa-Gómez

Posted Date: 24 January 2025

doi: 10.20944/preprints202501.1740.v1

Keywords: optimal area; T-shaped combined footings; minimum surface; surface works partially under compression

Preprints.org is a free multidisciplinary platform providing preprint service that is dedicated to making early versions of research outputs permanently available and citable. Preprints posted at Preprints.org appear in Web of Science, Crossref, Google Scholar, Scilit, Europe PMC.

Copyright: This open access article is published under a Creative Commons CC BY 4.0 license, which permit the free download, distribution, and reuse, provided that the author and preprint are cited in any reuse.

Preprints.org (www.preprints.org) | NOT PEER-REVIEWED | Posted: 24 January 2025 doi:10.20944/preprints202501.1740.v1

Disclaimer/Publisher's Note: The statements, opinions, and data contained in all publications are solely those of the individual author(s) and contributor(s) and not of MDPI and/or the editor(s). MDPI and/or the editor(s) disclaim responsibility for any injury to people or property resulting from any ideas, methods, instructions, or products referred to in the content.

Article

Mathematical Modeling for the Optimal Surface of T-Shaped Combined Footing Assuming That the Contact Area with the Ground Woks Partially Under Compression

Eyran Roberto Diaz-Gurrola [1], Arnulfo Luévanos-Rojas [1,*], Griselda Santiago-Hurtado [2], Victor Manuel Moreno-Landeros [1] and Aldo Emelio Landa-Gómez [3]

[1] Instituto de Investigaciones Multidisciplinaria, Universidad Autónoma de Coahuila, Blvd. Revolución No, 151 Ote, CP 27000, Torreón, Coahuila, Mexico

[2] Facultad de Ingeniería Civil, Universidad Autónoma de Coahuila, , CP 27276, Torreón, Coahuila, Mexico

[3] Facultad de Ingeniería Civil—Xalapa, Universidad Veracruzana, Lomas del Estadio S/N, Zona Universitaria, Xalapa CP 91000, Veracruz, Mexico

* Correspondence: arnulfoluevanos@uadec.edu.mx

Abstract: This study shows an optimal model to obtain the minimum contact surface with the ground for T-shaped combined footings, taking into account that the surface works partially under compression, this is, a part of the surface under the footing in contact with the ground is under compression and the other part the pressure is zero (linear pressure on the ground). There are works that show the minimum surface for T-shaped combined footings, but the surface beneath the footing in contact with the ground works entirely in compression. The model is developed by integration and/or by the geometric properties of a pyramid with a triangular-based to obtain the equations of the resultant force and the two moments (X and Y axes) for the fifteen cases of biaxial bending and three special cases of uniaxial bending (M_{y1} and M_{y2} are equals to zero). Three numerical examples are presented with the same data: Example 1 is for different bending moments; Example 2 is for bending moments M_{x1} and M_{x2} equals to zero; Example 3 is for bending moments M_{y1} and M_{y2} equals to zero. Also, a comparison is made with the current model (area works completely under compression) and the new model (area works partially under compression). The results show that savings of up to 31.40% can be achieved in the area of contact with the ground. In this way, the minimum surface model will be of great help to foundation engineering specialists.

Keywords: optimal area; T-shaped combined footings; minimum surface; surface works partially under compression

MSC: 32A40; 51E99; 90C90

1. Introduction

The ground pressure below a footing depends on the type of soil, the relative stiffness of the soil and the footing, and the depth of the foundation at the level of contact between the footing and the ground.

Figure 1 shows the distribution of ground pressure below of the contact surface of a footing depending on the ground type for a rigid footing. Figure 1(a) presents a rigid footing on sandy soil. Figure 1(b) shows a rigid footing on clay soil. Figure 1(c) presents the uniform distribution used in the current design [1].

© 2025 by the author(s). Distributed under a Creative Commons CC BY license.

Preprints.org (www.preprints.org) | NOT PEER-REVIEWED | Posted: 24 January 2025 doi:10.20944/preprints202501.1740.v1

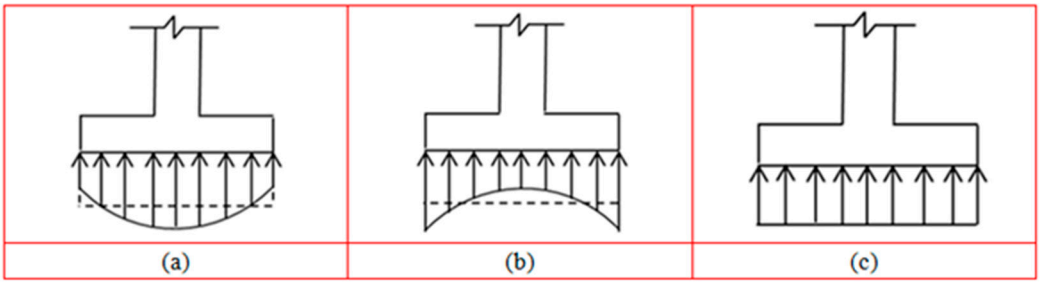

Figure 1. Distribution of the soil pressure below of a footing.

The proposed model considers that the distribution of the pressures on the ground is linear for T-shaped combined footings subjected to biaxial bending in each column.

The load capacity studies by analytical and/or experimental methods for different types of foundations have been investigated by several authors, such as: Shahin and Cheung [2], Dixit and Patil [3], ErzÍn and Gul [4], Colmenares *et al.* [5], Cure *et al*. [6], Fattah *et al.* [7], Uncuoğlu [8], Anil *et al.* [9], Khatri *et al.* [10], Mohebkhah [11], Zhang [12], Turedi *et al.* [13], Gnananandarao [14], Gör [15].

The most important investigations on rectangular isolated footings for the efficient management of soil-footing interaction problems have been carried out through the use of analytical methods [16–25], for graphics or design aids [26–28], and by analytical methods and graphics or design aids [29,30]. These documents are developed to obtain the axial load capacity and biaxial moment of the footing, or the pressure distribution in the contact area of a rigid rectangular isolated footing resting on the ground, and the dimensions of the footing are obtained through an iterative procedure.

The most important contributions on the studies of combined footings have been investigated by several researchers, such as: For rectangular footings by Maheshwari and Khatri [31], Konapure and Vivek [32], Vivek *et al*. [33], Ravi Kumar Reddy *et al*. [34], Kashani *et al*. [35]; For trapezoidal footings by Al-Douri [36], Luévanos-Rojas *et al*. [37]; T-shaped footings by Luévanos-Rojas *et al*. [38,39], Moreno-Landeros *et al*. [40]; For corner Footings by Aishwarya, K.M.; Balaji [41]; For strap footings by Luévanos-Rojas *et al*. [42].

The papers more related to this paper are: Luévanos-Rojas *et al.* [38] investigated an analytical model to obtain the dimensions of the reinforced concrete T-shaped combined footings in contact with the ground. Luévanos-Rojas *et al.* [39] proposed a design mathematical model to obtain the thickness and reinforcing steel for reinforced concrete T-shaped combined footings. Moreno-Landeros *et al*. [40] developed an optimal cost design for reinforced concrete T-shaped combined footings. All these works are developed under the criterion that the area of the footing works totally in compression.

Thus, the review of the previous studies shows that there are no works with the current level of knowledge on the minimum area of T-shaped combined footings, considering that the area works partially in compression.

This work presents an analytical model to obtain the minimum area for T-shaped combined footings assuming that the area in contact with the ground works partially in compression, i.e., a part of the footing contact area is subject to compression and another part without pressure (zero pressure). This paper shows the fifteen possible cases of footings subjected to biaxial bending and three special cases of uniaxial bending (M_{y1} and M_{y2} are equals to zero), and the resultant force R and the orthogonal moments on the X and Y axes are obtained by integration and are verified by the properties of a pyramid with a triangular base for biaxial bending and the properties of a triangular prism for uniaxial bending. Three numerical examples are presented in this paper. Example 1 is for biaxial bending; Example 2 is the same example 1, but M_{x1} and M_{x2} are equals to zero; Example 3 is the same example 1, but M_{y1} and M_{y2} are equals to zero. Each example presents four types of constraints, which are: Constraint 1 is for a footing with unconstrained sides; Constraint 2 is for a footing with one side constrained in column 1; Constraint 3 is for a footing with a side constrained in column 2; Constraint 4 is for a footing with two sides constrained (opposite sides). Also, a comparison is made with the current model (area works completely under compression) and the new model (area works partially under compression) to observe the different.

2. Formulation of the Model

Preprints.org (www.preprints.org) | NOT PEER-REVIEWED | Posted: 24 January 2025 doi:10.20944/preprints202501.1740.v1

This work makes the following considerations: the footing is supported on an elastic and homogeneous ground and the footing is totally rigid, i.e., the ground pressure on the footing behaves linearly.

Figure 2 shows a T-shaped combined footing (free sides at its ends) that supports two columns aligned on a Y axis (longitudinal axis), and each column transfers to the footing an axial load and two bending moments on the X and Y axes.

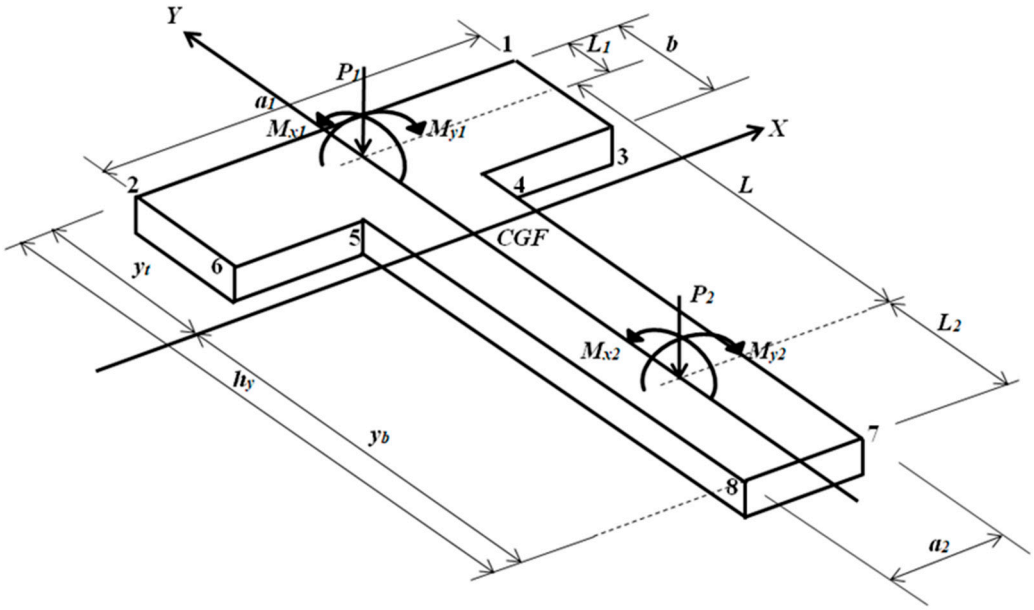

Figure 2. T-shaped combined footing with free sides.

The geometric properties of the T-shaped combined footing viewing in plan are:

$$A = (a_1 - a_2)b + a_2 h_y, \tag{1}$$

$$y_t = \frac{(a_1 - a_2)b^2 + a_2 {h_y}^2}{2\left[(a_1 - a_2)b + a_2 h_y\right]}, \tag{2}$$

$$y_b = \frac{(2h_y - b)(a_1 - a_2)b + a_2 {h_y}^2}{2\left[(a_1 - a_2)b + a_2 h_y\right]}, \tag{3}$$

$$I_x = \frac{a_2 h_y b(a_1 - a_2)(h_y - b)^2\left[a_2 h_y + b(a_1 - a_2)\right]}{4\left[(a_1 - a_2)b + a_2 h_y\right]^2} + \frac{(a_1 - a_2)b^3 + a_2 {h_y}^3}{12}, \tag{4}$$

$$I_y = \frac{b{a_1}^3 + (h_y - b){a_2}^3}{12}, \tag{5}$$

where: A = Area of the footing in plan (m²), y_t = Distance from center of footing to positive end (m), y_b = Distance from center of footing to negative end (m), I_x = Moment of inertia about the X axis (m⁴), I_y = Moment of inertia about the Y axis (m⁴).

2.1. Biaxial Bending

In this subsection, the fifteen possible cases for a T-shaped combined footing subjected to axial load and two orthogonal bending moments in each column are presented.

Preprints.org (www.preprints.org) | NOT PEER-REVIEWED | Posted: 24 January 2025 doi:10.20944/preprints202501.1740.v1

For case I, it is assumed that the entire bottom surface of the footing works under compression. The pressures generated by the ground on the footing are obtained by the following equation (biaxial bending equation):

$$\sigma = \frac{R}{A} + \frac{M_{xT}y}{I_x} + \frac{M_{yT}x}{I_y}. \quad (6)$$

where: σ = Allowable soil pressure (kN/m²), M_x = Bending moment about X axis (kN-m), M_y = Bending moment about Y axis (kN-m).

Note: R, M_x and M_y can be determined as follows:

$$R = P_1 + P_2, \quad (7)$$

$$M_{xT} = M_{x1} + M_{x2} + P_1(y_t - L_1) - P_2(h_y - y_t - L_2), \quad (8)$$

$$M_{yT} = M_{y1} + M_{y2}. \quad (9)$$

For cases II to XV, it is assumed that the entire bottom surface of the footing works partially under compression, i.e., part of the contact area there is no pressure, and by integration and/or by the geometric properties of a pyramid with a triangular base, the resultant force R, the moment on the X axis M_{xT} and the moment on the Y axis M_{yT} are obtained.

The pressures generated by the ground on the footing are obtained by means of the general equation of the pressure plane, starting from three known points.

The general equation of a 3-D pressure plane of the ground on the footing is:

$$Ax + By + C\sigma_z + D = 0. \quad (10)$$

For cases II to XV, the three known points of the pressure plane are:

$$p_1\left(\frac{a_1}{2}, y_t, \sigma_{max}\right);\ p_2\left(\frac{a_1}{2} - L_{x1}, y_t, 0\right);\ p_3\left(\frac{a_1}{2}, y_t - L_{y1}, 0\right). \quad (11)$$

The general equation of the pressure plane is obtained as follows:

$$\begin{vmatrix} x - \left(\frac{a_1}{2}\right) & y - (y_t) & \sigma_z - \sigma_{max} \\ \frac{a_1}{2} - L_{x1} - \left(\frac{a_1}{2}\right) & y_t - (y_t) & 0 - \sigma_{max} \\ \frac{a_1}{2} - \left(\frac{a_1}{2}\right) & y_t - L_{y1} - (y_t) & 0 - \sigma_{max} \end{vmatrix}. \quad (12)$$

Solving the determinant of Equation (12) gives the pressure at any point σ_z:

$$\sigma_z = \frac{\sigma_{max}\left[2L_{x1}(L_{y1} + y - y_t) + L_{y1}(2x - a_1)\right]}{2L_{x1}L_{y1}}. \quad (13)$$

The equation of the straight line that forms the neutral axis is:

$$2L_{x1}(L_{y1} + y - y_t) + L_{y1}(2x - a_1) = 0. \quad (14)$$

Figure 3 shows Case I assuming that the entire bottom surface of the footing works under compression.

Preprints.org (www.preprints.org) | NOT PEER-REVIEWED | Posted: 24 January 2025 doi:10.20944/preprints202501.1740.v1

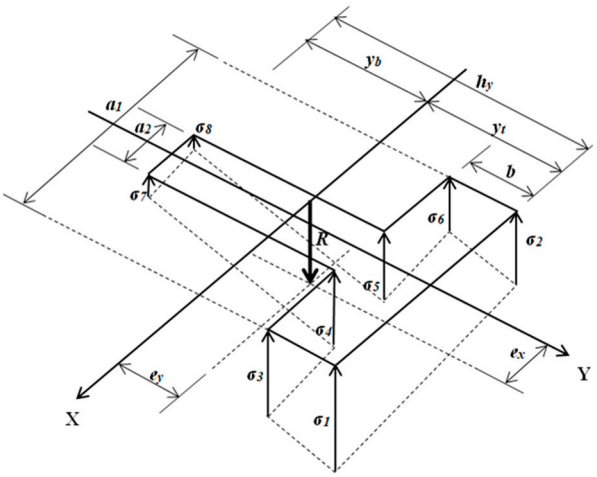

Figure 3. Case I.

Figure 4 shows Cases II to XV assuming that the entire bottom surface of the footing works partially under compression.

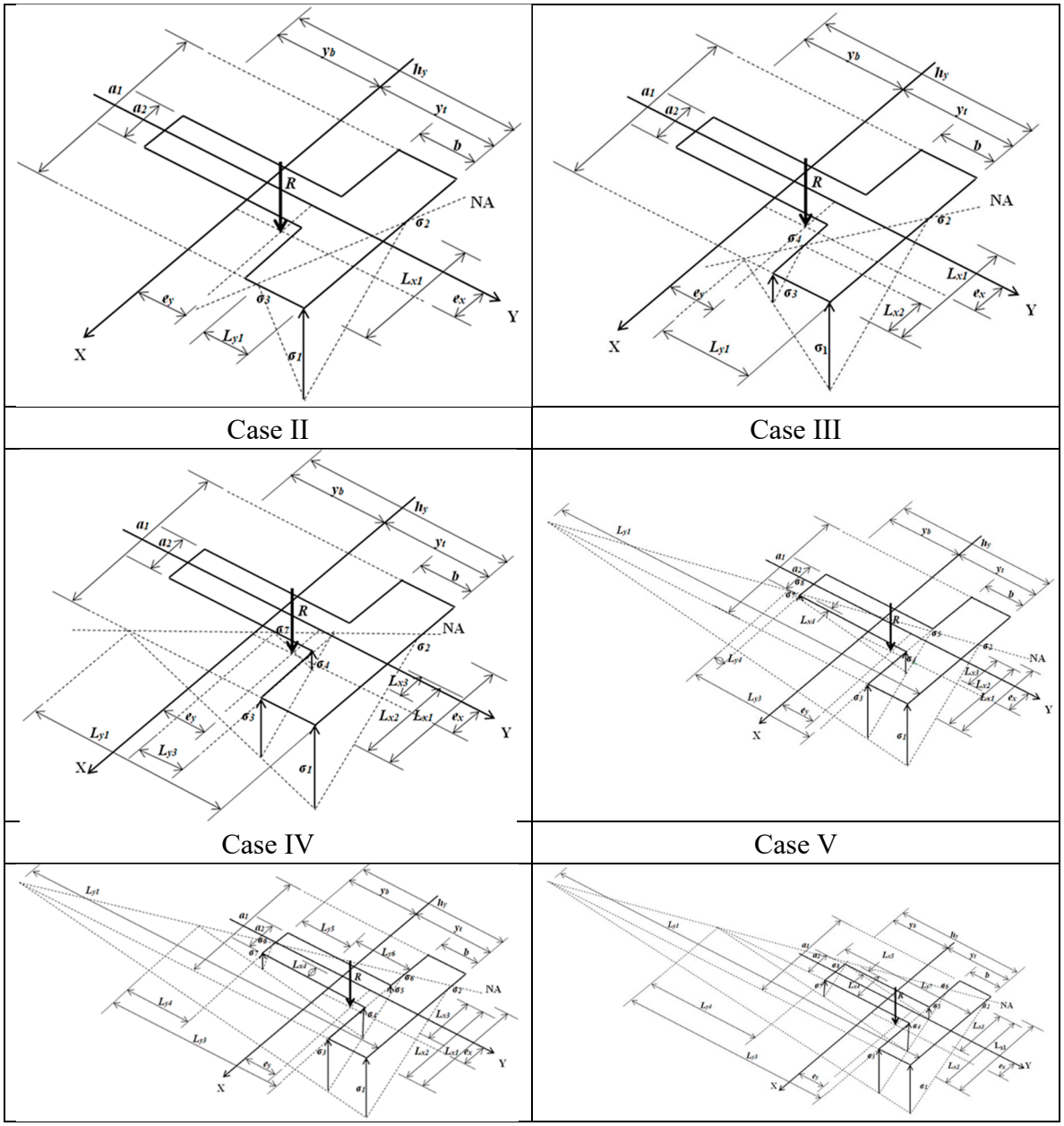

Preprints.org (www.preprints.org) | NOT PEER-REVIEWED | Posted: 24 January 2025 doi:10.20944/preprints202501.1740.v1

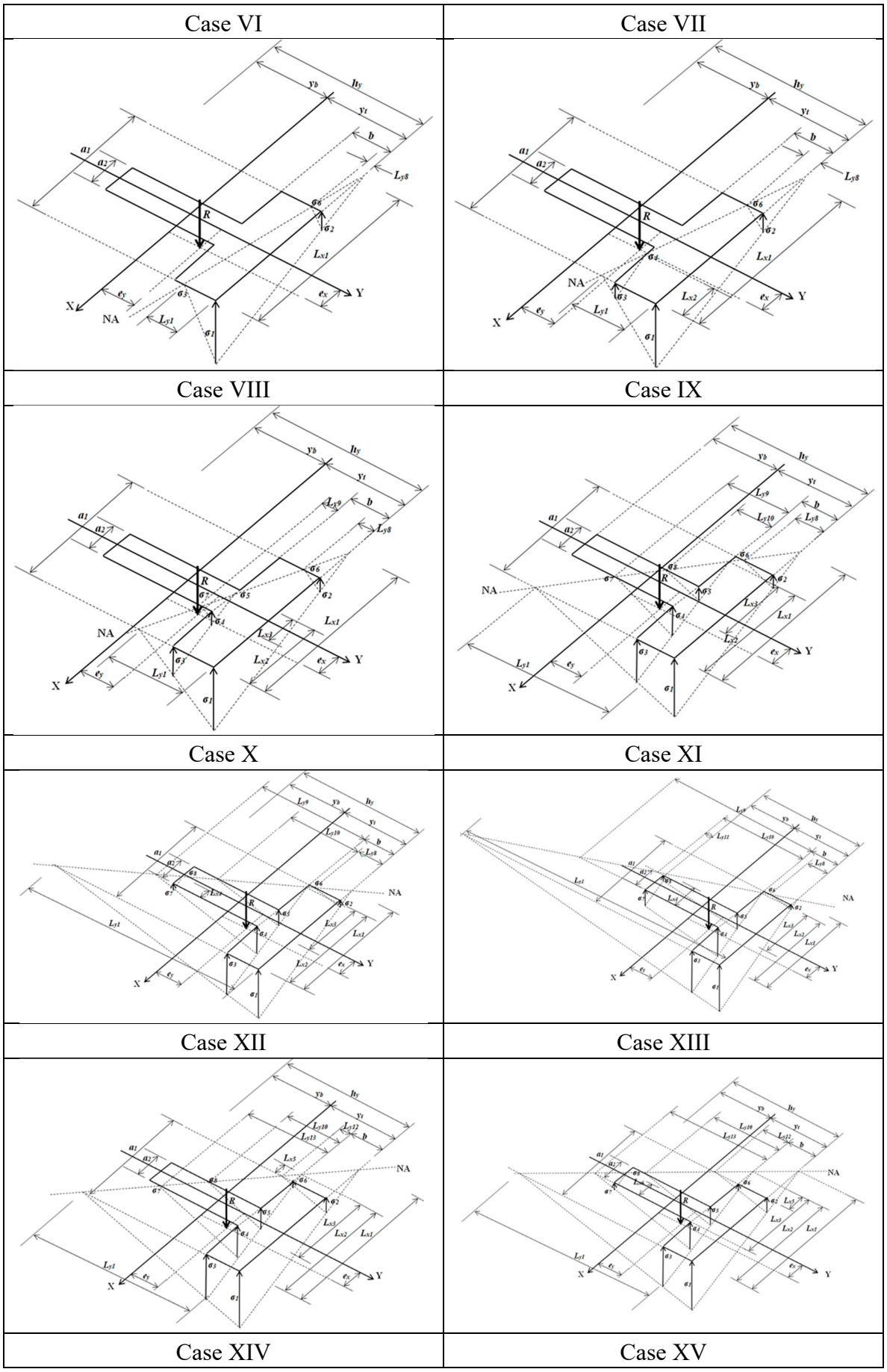

Figure 4. Cases II to XV.

Preprints.org (www.preprints.org) | NOT PEER-REVIEWED | Posted: 24 January 2025 doi:10.20944/preprints202501.1740.v1

2.1.1. Case I

The general equations for the soil pressure at each vertex of a footing subjected to biaxial bending are obtained from equation (6) as follows:

$$\sigma_1 = \frac{R}{A} + \frac{M_{xT} y_t}{I_x} + \frac{M_{yT} a_1}{2I_y}, \tag{15}$$

$$\sigma_2 = \frac{R}{A} + \frac{M_{xT} y_t}{I_x} - \frac{M_{yT} a_1}{2I_y}, \tag{16}$$

$$\sigma_3 = \frac{R}{A} + \frac{M_{xT} (y_t - b)}{I_x} + \frac{M_{yT} a_1}{2I_y}, \tag{17}$$

$$\sigma_4 = \frac{R}{A} + \frac{M_{xT} (y_t - b)}{I_x} + \frac{M_{yT} a_2}{2I_y}, \tag{18}$$

$$\sigma_5 = \frac{R}{A} + \frac{M_{xT} (y_t - b)}{I_x} - \frac{M_{yT} a_2}{2I_y}, \tag{19}$$

$$\sigma_6 = \frac{R}{A} + \frac{M_{xT} (y_t - b)}{I_x} - \frac{M_{yT} a_1}{2I_y}, \tag{20}$$

$$\sigma_7 = \frac{R}{A} - \frac{M_{xT} (h_y - y_t)}{I_x} + \frac{M_{yT} a_2}{2I_y}, \tag{21}$$

$$\sigma_8 = \frac{R}{A} - \frac{M_{xT} (h_y - y_t)}{I_x} - \frac{M_{yT} a_2}{2I_y}. \tag{22}$$

The general equations of R, M_{xT} and M_{yT} for cases II to XV are presented below.

2.1.2. Case II

$$R = \int_{y_t - L_{y1}}^{y_t} \int_{\frac{a_1}{2} + \frac{(y_t - L_{y1} - y) L_{x1}}{L_{y1}}}^{\frac{a_1}{2}} \sigma_z dx dy, \tag{23}$$

$$R = \frac{\sigma_{max} L_{x1} L_{y1}}{6}, \tag{24}$$

$$M_{xT} = \int_{y_t - L_{y1}}^{y_t} \int_{\frac{a_1}{2} + \frac{(y_t - L_{y1} - y) L_{x1}}{L_{y1}}}^{\frac{a_1}{2}} \sigma_z y dx dy, \tag{25}$$

$$M_{xT} = \frac{\sigma_{max} L_{x1} L_{y1} (4y_t - L_{y1})}{24}, \tag{26}$$

$$M_{yT} = \int_{y_t - L_{y1}}^{y_t} \int_{\frac{a_1}{2} + \frac{(y_t - L_{y1} - y) L_{x1}}{L_{y1}}}^{\frac{a_1}{2}} \sigma_z x dx dy, \tag{27}$$

Preprints.org (www.preprints.org) | NOT PEER-REVIEWED | Posted: 24 January 2025 doi:10.20944/preprints202501.1740.v1

$$M_{yT} = \frac{\sigma_{max} L_{x1} L_{y1} (2a_1 - L_{x1})}{24}. \tag{28}$$

2.1.3. Case III

$$R = \int_{y_t - b}^{y_t} \int_{\frac{a_1}{2} + \frac{(y_t - L_{y1} - y) L_{x1}}{L_{y1}}}^{\frac{a_1}{2}} \sigma_z dx dy, \tag{29}$$

$$R = \frac{\sigma_{max} L_{x1} \left[{L_{y1}}^3 - \left(L_{y1} - b \right)^3 \right]}{6 {L_{y1}}^2}, \tag{30}$$

$$M_{xT} = \int_{y_t - b}^{y_t} \int_{\frac{a_1}{2} + \frac{(y_t - L_{y1} - y) L_{x1}}{L_{y1}}}^{\frac{a_1}{2}} \sigma_z y dx dy, \tag{31}$$

$$M_{xT} = \frac{\sigma_{max} L_{x1} \left[{L_{y1}}^3 (4y_t - L_{y1}) - \left(L_{y1} - b \right)^3 (4y_t - 3b - L_{y1}) \right]}{24 {L_{y1}}^2}, \tag{32}$$

$$M_{yT} = \int_{y_t - b}^{y_t} \int_{\frac{a_1}{2} + \frac{(y_t - L_{y1} - y) L_{x1}}{L_{y1}}}^{\frac{a_1}{2}} \sigma_z x dx dy, \tag{33}$$

$$M_{yT} = \frac{\sigma_{max} L_{x1} \left\{ {L_{y1}}^4 (2a_1 - L_{x1}) - \left(L_{y1} - b \right)^3 \left[2a_1 L_{y1} - L_{x1} \left(L_{y1} - b \right) \right] \right\}}{24 {L_{y1}}^3}. \tag{34}$$

2.1.4. Case IV

$$\begin{aligned} R = & \int_{y_t - b}^{y_t} \int_{\frac{a_1}{2} + \frac{(y_t - L_{y1} - y) L_{x1}}{L_{y1}}}^{\frac{a_1}{2}} \sigma_z dx dy \\ & + \int_{y_t - b - \frac{2L_{x1}(L_{y1} - b) - L_{y1}(a_1 - a_2)}{2L_{x1}}}^{y_t - b} \int_{\frac{a_1}{2} + \frac{(y_t - L_{y1} - y) L_{x1}}{L_{y1}}}^{\frac{a_2}{2}} \sigma_z dx dy, \end{aligned} \tag{35}$$

$$R = \frac{\sigma_{max} \left\{ 8 {L_{x1}}^3 \left[{L_{y1}}^3 - \left(L_{y1} - b \right)^3 \right] + \left[2L_{x1} \left(L_{y1} - b \right) - L_{y1} (a_1 - a_2) \right]^3 \right\}}{48 {L_{x1}}^2 {L_{y1}}^2}, \tag{36}$$

$$\begin{aligned} M_{xT} = & \int_{y_t - b}^{y_t} \int_{\frac{a_1}{2} + \frac{(y_t - L_{y1} - y) L_{x1}}{L_{y1}}}^{\frac{a_1}{2}} \sigma_z y dx dy \\ & + \int_{y_t - b - \frac{2L_{x1}(L_{y1} - b) - L_{y1}(a_1 - a_2)}{2L_{x1}}}^{y_t - b} \int_{\frac{a_1}{2} + \frac{(y_t - L_{y1} - y) L_{x1}}{L_{y1}}}^{\frac{a_2}{2}} \sigma_z y dx dy, \end{aligned} \tag{37}$$

Preprints.org (www.preprints.org) | NOT PEER-REVIEWED | Posted: 24 January 2025 doi:10.20944/preprints202501.1740.v1

$$M_{xT} = \frac{\sigma_{max}\left[2L_{x1}(L_{y1}-b)-L_{y1}(a_1-a_2)\right]^3\left[2L_{x1}(4y_t-3b-L_{y1})+L_{y1}(a_1-a_2)\right]}{384{L_{x1}}^3{L_{y1}}^2} + \frac{\sigma_{max}L_{x1}\left[{L_{y1}}^3(4y_t-L_{y1})-(L_{y1}-b)^3(4y_t-3b-L_{y1})\right]}{24{L_{y1}}^2}, \quad (38)$$

$$M_{yT} = \int_{y_t-b}^{y_t}\int_{\frac{a_1}{2}+\frac{(y_t-L_{y1}-y)L_{x1}}{L_{y1}}}^{\frac{a_1}{2}}\sigma_z x\,dx\,dy + \int_{y_t-b-\frac{2L_{x1}(L_{y1}-b)-L_{y1}(a_1-a_2)}{2L_{x1}}}^{y_t-b}\int_{\frac{a_1}{2}+\frac{(y_t-L_{y1}-y)L_{x1}}{L_{y1}}}^{\frac{a_2}{2}}\sigma_z x\,dx\,dy, \quad (39)$$

$$M_{yT} = \frac{\sigma_{max}\left[2L_{x1}(L_{y1}-b)-L_{y1}(a_1-a_2)\right]^3\left[L_{y1}(a_1+3a_2)-2L_{x1}(L_{y1}-b)\right]}{384{L_{x1}}^2{L_{y1}}^3} + \frac{\sigma_{max}L_{x1}\left\{{L_{y1}}^4(2a_1-L_{x1})-(L_{y1}-b)^3\left[2a_1L_{y1}-L_{x1}(L_{y1}-b)\right]\right\}}{24{L_{y1}}^3}, \quad (40)$$

2.1.5. Case V

$$R = \int_{y_t-b}^{y_t}\int_{\frac{a_1}{2}+\frac{(y_t-L_{y1}-y)L_{x1}}{L_{y1}}}^{\frac{a_1}{2}}\sigma_z\,dx\,dy + \int_{y_t-hy}^{y_t-b}\int_{\frac{a_1}{2}+\frac{(y_t-L_{y1}-y)L_{x1}}{L_{y1}}}^{\frac{a_2}{2}}\sigma_z\,dx\,dy, \quad (41)$$

$$R = \frac{\sigma_{max}\left\{8{L_{x1}}^3\left[{L_{y1}}^3-(L_{y1}-b)^3\right]+\left[2L_{x1}(L_{y1}-b)-L_{y1}(a_1-a_2)\right]^3-\left[2L_{x1}(L_{y1}- \right.\right.}{48{L_{x1}}^2{L_{y1}}^2} \quad (42)$$

$$M_{xT} = \int_{y_t-b}^{y_t}\int_{\frac{a_1}{2}+\frac{(y_t-L_{y1}-y)L_{x1}}{L_{y1}}}^{\frac{a_1}{2}}\sigma_z y\,dx\,dy + \int_{y_t-hy}^{y_t-b}\int_{\frac{a_1}{2}+\frac{(y_t-L_{y1}-y)L_{x1}}{L_{y1}}}^{\frac{a_2}{2}}\sigma_z y\,dx\,dy, \quad (43)$$

$$M_{xT} = \frac{\sigma_{max}\left\{\left[2L_{x1}(L_{y1}-b)-L_{y1}(a_1-a_2)\right]^3\right\}\left[(4y_t-3b-L_{y1})+L_{y1}(a_1-a_2)\right]}{384{L_{x1}}^3{L_{y1}}^2} - \frac{\sigma_{max}\left[2L_{x1}(L_{y1}-h_y)-L_{y1}(a_1-a_2)\right]^3\left[(4y_t-3h_y-L_{y1})+L_{y1}(a_1-a_2)\right]}{384{L_{x1}}^3{L_{y1}}^2} + \frac{\sigma_{max}L_{x1}\left[{L_{y1}}^3(4y_t-L_{y1})-(L_{y1}-b)^3(4y_t-3b-L_{y1})\right]}{24{L_{y1}}^2}, \quad (44)$$

$$M_{yT} = \int_{y_t-b}^{y_t}\int_{\frac{a_1}{2}+\frac{(y_t-L_{y1}-y)L_{x1}}{L_{y1}}}^{\frac{a_1}{2}}\sigma_z x\,dx\,dy + \int_{y_t-hy}^{y_t-b}\int_{\frac{a_1}{2}+\frac{(y_t-L_{y1}-y)L_{x1}}{L_{y1}}}^{\frac{a_2}{2}}\sigma_z x\,dx\,dy, \quad (45)$$

Preprints.org (www.preprints.org) | NOT PEER-REVIEWED | Posted: 24 January 2025 doi:10.20944/preprints202501.1740.v1

$$M_{yT} = \frac{\sigma_{max}\left[2L_{x1}(L_{y1}-b)-L_{y1}(a_1-a_2)\right]^3\left[L_{y1}(a_1+3a_2)-2L_{x1}(L_{y1}-b)\right]}{384{L_{x1}}^2{L_{y1}}^3} - \frac{\sigma_{max}\left[2L_{x1}(L_{y1}-h_y)-L_{y1}(a_1-a_2)\right]^3\left[L_{y1}(a_1+3a_2)-2L_{x1}(L_{y1}-h_y)\right]}{384{L_{x1}}^2{L_{y1}}^3} + \frac{\sigma_{max}L_{x1}\left\{{L_{y1}}^4(2a_1-L_{x1})-\left(L_{y1}-b\right)^3\left[2a_1L_{y1}-L_{x1}(L_{y1}-b)\right]\right\}}{24{L_{y1}}^3}. \quad (46)$$

2.1.6. Case VI

$$R = \int_{y_t-b}^{y_t-b-\frac{2L_{x1}(L_{y1}-b)-L_{y1}(a_1+a_2)}{2L_{x1}}}\int_{-\frac{a_2}{2}}^{\frac{a_2}{2}}\sigma_z dxdy + \int_{y_t-hy}^{y_t-b-\frac{2L_{x1}(L_{y1}-b)-L_{y1}(a_1+a_2)}{2L_{x1}}}\int_{\frac{a_1}{2}+\frac{(y_t-L_{y1}-y)L_{x1}}{L_{y1}}}^{\frac{a_2}{2}}\sigma_z dxdy + \int_{y_t-b}^{y_t}\int_{\frac{a_1}{2}+\frac{(y_t-L_{y1}-y)L_{x1}}{L_{y1}}}^{\frac{a_1}{2}}\sigma_z dxdy, \quad (47)$$

$$R = \frac{\sigma_{max}\left\{2{L_{y1}}^3\left[4{L_{x1}}^3+a_2(3{a_1}^2+{a_2}^2)\right]-8L_{x1}(L_{y1}-b)\left\{{L_{x1}}^2(L_{y1}-b)^2-3a_2L_{y1}\right[}{48{L_{x1}}^2{L_{y1}}^2} - \frac{\sigma_{max}\left[2L_{x1}(L_{y1}-h_y)-L_{y1}(a_1-a_2)\right]^3}{48{L_{x1}}^2{L_{y1}}^2}, \quad (48)$$

$$M_{xT} = \int_{y_t-b}^{y_t-b-\frac{2L_{x1}(L_{y1}-b)-L_{y1}(a_1+a_2)}{2L_{x1}}}\int_{-\frac{a_2}{2}}^{\frac{a_2}{2}}\sigma_z y dxdy + \int_{y_t-hy}^{y_t-b-\frac{2L_{x1}(L_{y1}-b)-L_{y1}(a_1+a_2)}{2L_{x1}}}\int_{\frac{a_1}{2}+\frac{(y_t-L_{y1}-y)L_{x1}}{L_{y1}}}^{\frac{a_2}{2}}\sigma_z y dxdy + \int_{y_t-b}^{y_t}\int_{\frac{a_1}{2}+\frac{(y_t-L_{y1}-y)L_{x1}}{L_{y1}}}^{\frac{a_1}{2}}\sigma_z y dxdy, \quad (49)$$

Preprints.org (www.preprints.org) | NOT PEER-REVIEWED | Posted: 24 January 2025 doi:10.20944/preprints202501.1740.v1

$$M_{xT} = \frac{\sigma_{max} L_{x1} L_{y1}(4y_t - L_{y1})}{24} - \frac{\sigma_{max}\left[2L_{x1}(L_{y1} - h_y) - L_{y1}(a_1 - a_2)\right]^3\left[2L_{x1}(4y_t - 3h_y - L_{y1}) + L_{y1}(a_1 - a_2)\right]}{384 {L_{x1}}^3 {L_{y1}}^2} - \frac{\sigma_{max}(4y_t - 3b - L_{y1})\left\{4{L_{x1}}^3(L_{y1} - b)^3 - 3L_{y1}a_2\left[2L_{x1}(L_{y1} - b) - L_{y1}a_1\right]^2 - L_{y1}\right.}{96 {L_{x1}}^2 {L_{y1}}^2} - \frac{\sigma_{max} a_2\left\{4\left[L_{x1}(L_{y1} - b) - L_{y1}a_1\right]^3 - {L_{y1}}^2({a_1}^2 - {a_2}^2)\left[3L_{x1}(L_{y1} - b) - 2L_{y1}a_1\right]\right\}}{96 {L_{x1}}^3 L_{y1}}, \quad (50)$$

$$M_{yT} = \int_{y_t - b - \frac{2L_{x1}(L_{y1} - b) - L_{y1}(a_1 + a_2)}{2L_{x1}}}^{y_t - b} \int_{-\frac{a_2}{2}}^{\frac{a_2}{2}} \sigma_z x dx dy + \int_{y_t - hy}^{y_t - b - \frac{2L_{x1}(L_{y1} - b) - L_{y1}(a_1 + a_2)}{2L_{x1}}} \int_{\frac{a_1}{2} + \frac{(y_t - L_{y1} - y)L_{x1}}{L_{y1}}}^{\frac{a_2}{2}} \sigma_z x dx dy + \int_{y_t - b}^{y_t} \int_{\frac{a_1}{2} + \frac{(y_t - L_{y1} - y)L_{x1}}{L_{y1}}}^{\frac{a_1}{2}} \sigma_z x dx dy, \quad (51)$$

$$M_{yT} = \frac{\sigma_{max}\left\{{L_{x1}}^3 {L_{y1}}^4(2a_1 - L_{x1}) - {L_{x1}}^3(L_{y1} - b)^3\left[2a_1 L_{y1} - L_{x1}(L_{y1} - b)\right] - {L_{y1}}^3 {a_2}^3[I\right.}{24 {L_{x1}}^2 {L_{y1}}^3} - \frac{\sigma_{max}\left[2L_{x1}(L_{y1} - h_y) - L_{y1}(a_1 - a_2)\right]^3\left[L_{y1}(a_1 + 3a_2) - 2L_{x1}(L_{y1} - h_y)\right]}{384 {L_{x1}}^2 {L_{y1}}^3}. \quad (52)$$

2.1.7. Case VII

$$R = \int_{y_t - b}^{y_t} \int_{\frac{a_1}{2} + \frac{(y_t - L_{y1} - y)L_{x1}}{L_{y1}}}^{\frac{a_1}{2}} \sigma_z dx dy + \int_{y_t - hy}^{y_t - b} \int_{-\frac{a_2}{2}}^{\frac{a_2}{2}} \sigma_z dx dy, \quad (53)$$

$$R = \frac{\sigma_{max}\left\{{L_{x1}}^2\left[{L_{y1}}^3 + (b - L_{y1})^3\right] + 3L_{y1}a_2(b - h_y)\left[L_{y1}a_1 - L_{x1}(2L_{y1} - b - h_y)\right]\right\}}{6 L_{x1} {L_{y1}}^2}, \quad (54)$$

$$M_{xT} = \int_{y_t - b}^{y_t} \int_{\frac{a_1}{2} + \frac{(y_t - L_{y1} - y)L_{x1}}{L_{y1}}}^{\frac{a_1}{2}} \sigma_z y dx dy + \int_{y_t - hy}^{y_t - b} \int_{-\frac{a_2}{2}}^{\frac{a_2}{2}} \sigma_z y dx dy, \quad (55)$$

Preprints.org (www.preprints.org) | NOT PEER-REVIEWED | Posted: 24 January 2025 doi:10.20944/preprints202501.1740.v1

$$M_{xT} = \frac{\sigma_{max} a_2 {L_{x1}}^2 (h_y - b)\{4L_{x1}(b^2 + bh_y + {h_y}^2) + 3L_{y1}(a_1 - 2L_{x1})(b + h_y) - 6y_t[L_{x1}}{12{L_{x1}}^3 L_{y1}} + \frac{\sigma_{max} L_{x1}\left[{L_{y1}}^3(4y_t - L_{y1}) - (L_{y1} - b)^3(4y_t - 3b - L_{y1})\right]}{24{L_{y1}}^2}, \quad (56)$$

$$M_{yT} = \int_{y_t - b}^{y_t} \int_{\frac{a_1}{2} + \frac{(y_t - L_{y1} - y)L_{x1}}{L_{y1}}}^{\frac{a_1}{2}} \sigma_z x dx dy + \int_{y_t - hy}^{y_t - b} \int_{-\frac{a_2}{2}}^{\frac{a_2}{2}} \sigma_z x dx dy, \quad (57)$$

$$M_{yT} = \frac{\sigma_{max}\left\{{L_{x1}}^3\left[(b - L_{y1})^4 - {L_{y1}}^4\right] + 2L_{x1} b L_{y1} a_1\left[b^2 - 3L_{y1}(b - L_{y1})\right] - 2{a_2}^3{L_{y1}}^3(b\right.}{24L_{x1}{L_{y1}}^3} \quad (58)$$

2.1.8. Case VIII

$$R = \int_{y_t - \frac{L_{y1}(L_{x1} - a_1)}{L_{x1}}}^{y_t} \int_{-\frac{a_1}{2}}^{\frac{a_1}{2}} \sigma_z dx dy + \int_{y_t - L_{y1}}^{y_t - \frac{L_{y1}(L_{x1} - a_1)}{L_{x1}}} \int_{\frac{a_1}{2} + \frac{(y_t - L_{y1} - y)L_{x1}}{L_{y1}}}^{\frac{a_1}{2}} \sigma_z dx dy, \quad (59)$$

$$R = \frac{\sigma_{max} L_{y1}\left[{L_{x1}}^3 - (L_{x1} - a_1)^3\right]}{6{L_{x1}}^2}, \quad (60)$$

$$M_{xT} = \int_{y_t - \frac{L_{y1}(L_{x1} - a_1)}{L_{x1}}}^{y_t} \int_{-\frac{a_1}{2}}^{\frac{a_1}{2}} \sigma_z y dx dy + \int_{y_t - L_{y1}}^{y_t - \frac{L_{y1}(L_{x1} - a_1)}{L_{x1}}} \int_{\frac{a_1}{2} + \frac{(y_t - L_{y1} - y)L_{x1}}{L_{y1}}}^{\frac{a_1}{2}} \sigma_z y dx dy, \quad (61)$$

$$M_{xT} = \frac{\sigma_{max} L_{y1}\left[{L_{x1}}^4(4y_t - L_{y1}) - (L_{x1} - a_1)^3\left[4L_{x1} y_t - L_{y1}(L_{x1} - a_1)\right]\right]}{24{L_{x1}}^3}, \quad (62)$$

$$M_{yT} = \int_{y_t - \frac{L_{y1}(L_{x1} - a_1)}{L_{x1}}}^{y_t} \int_{-\frac{a_1}{2}}^{\frac{a_1}{2}} \sigma_z x dx dy + \int_{y_t - L_{y1}}^{y_t - \frac{L_{y1}(L_{x1} - a_1)}{L_{x1}}} \int_{\frac{a_1}{2} + \frac{(y_t - L_{y1} - y)L_{x1}}{L_{y1}}}^{\frac{a_1}{2}} \sigma_z x dx dy, \quad (63)$$

$$M_{yT} = \frac{\sigma_{max} {a_1}^3 L_{y1}(2L_{x1} - a_1)}{24{L_{x1}}^2}. \quad (64)$$

2.1.9. Case IX

$$R = \int_{y_t - \frac{L_{y1}(L_{x1} - a_1)}{L_{x1}}}^{y_t} \int_{-\frac{a_1}{2}}^{\frac{a_1}{2}} \sigma_z dx dy + \int_{y_t - b}^{y_t - \frac{L_{y1}(L_{x1} - a_1)}{L_{x1}}} \int_{\frac{a_1}{2} + \frac{(y_t - L_{y1} - y)L_{x1}}{L_{y1}}}^{\frac{a_1}{2}} \sigma_z dx dy, \quad (65)$$

$$R = \frac{\sigma_{max}\left\{{L_{y1}}^3\left[{L_{x1}}^3 - (L_{x1} - a_1)^3\right] - {L_{x1}}^3(L_{y1} - b)^3\right\}}{6{L_{x1}}^2{L_{y1}}^2}, \quad (66)$$

Preprints.org (www.preprints.org) | NOT PEER-REVIEWED | Posted: 24 January 2025 doi:10.20944/preprints202501.1740.v1

$$M_{xT} = \int_{y_t-\frac{L_{y1}(L_{x1}-a_1)}{L_{x1}}}^{y_t} \int_{-\frac{a_1}{2}}^{\frac{a_1}{2}} \sigma_z y dx dy + \int_{y_t-b}^{y_t-\frac{L_{y1}(L_{x1}-a_1)}{L_{x1}}} \int_{\frac{a_1}{2}+\frac{(y_t-L_{y1}-y)L_{x1}}{L_{y1}}}^{\frac{a_1}{2}} \sigma_z y dx dy, \quad (67)$$

$$M_{xT} = \frac{\sigma_{max}\left\{{L_{y1}}^3\left\{{L_{x1}}^4(4y_t - L_{y1}) - (L_{x1}-a_1)^3\left[4L_{x1}y_t - L_{y1}(L_{x1}-a_1)\right]\right\} - {L_{x1}}^4\left(L_{y1} - \right.\right.}{24{L_{x1}}^3{L_{y1}}^2} \quad (68)$$

$$M_{yT} = \int_{y_t-\frac{L_{y1}(L_{x1}-a_1)}{L_{x1}}}^{y_t} \int_{-\frac{a_1}{2}}^{\frac{a_1}{2}} \sigma_z x dx dy + \int_{y_t-b}^{y_t-\frac{L_{y1}(L_{x1}-a_1)}{L_{x1}}} \int_{\frac{a_1}{2}+\frac{(y_t-L_{y1}-y)L_{x1}}{L_{y1}}}^{\frac{a_1}{2}} \sigma_z x dx dy, \quad (69)$$

$$M_{yT} = \frac{\sigma_{max}\left\{{a_1}^3{L_{y1}}^4(2L_{x1}-a_1) - {L_{x1}}^3\left(L_{y1}-b\right)^3\left[2L_{y1}a_1 - L_{x1}\left(L_{y1}-b\right)\right]\right\}}{24{L_{x1}}^2{L_{y1}}^3}. \quad (70)$$

2.1.10. Case X

$$R = \int_{y_t-\frac{L_{y1}(L_{x1}-a_1)}{L_{x1}}}^{y_t} \int_{-\frac{a_1}{2}}^{\frac{a_1}{2}} \sigma_z dx dy + \int_{y_t-b}^{y_t-\frac{L_{y1}(L_{x1}-a_1)}{L_{x1}}} \int_{\frac{a_1}{2}+\frac{(y_t-L_{y1}-y)L_{x1}}{L_{y1}}}^{\frac{a_1}{2}} \sigma_z dx dy + \int_{y_t-b-\frac{2L_{x1}(L_{y1}-b)-L_{y1}(a_1-a_2)}{2L_{x1}}}^{y_t-b} \int_{\frac{a_1}{2}+\frac{(y_t-L_{y1}-y)L_{x1}}{L_{y1}}}^{\frac{a_2}{2}} \sigma_z dx dy, \quad (71)$$

$$R = \frac{\sigma_{max}\left\{8{L_{y1}}^3\left[{L_{x1}}^3 - (L_{x1}-a_1)^3\right] - {L_{x1}}^3\left(L_{y1}-b\right)^3 + \left[2L_{x1}\left(L_{y1}-b\right) - L_{y1}(a_1-a\right.\right.}{48{L_{x1}}^2{L_{y1}}^2} \quad (72)$$

$$M_{xT} = \int_{y_t-\frac{L_{y1}(L_{x1}-a_1)}{L_{x1}}}^{y_t} \int_{-\frac{a_1}{2}}^{\frac{a_1}{2}} \sigma_z y dx dy + \int_{y_t-b}^{y_t-\frac{L_{y1}(L_{x1}-a_1)}{L_{x1}}} \int_{\frac{a_1}{2}+\frac{(y_t-L_{y1}-y)L_{x1}}{L_{y1}}}^{\frac{a_1}{2}} \sigma_z y dx dy + \int_{y_t-b-\frac{2L_{x1}(L_{y1}-b)-L_{y1}(a_1-a_2)}{2L_{x1}}}^{y_t-b} \int_{\frac{a_1}{2}+\frac{(y_t-L_{y1}-y)L_{x1}}{L_{y1}}}^{\frac{a_2}{2}} \sigma_z y dx dy, \quad (73)$$

$$M_{xT} = \frac{\sigma_{max}\left\{{L_{y1}}^3 a_1\left[L_{x1}\left(3{L_{x1}}^2 - 3L_{x1}a_1 + {a_1}^2\right)(4y_t - L_{y1}) - L_{y1}(L_{x1}-a_1)^3\right] - {L_{x1}}^4\left(L_y\right.\right.}{24{L_{x1}}^3{L_{y1}}^2} + \frac{\sigma_{max}\left[2L_{x1}\left(L_{y1}-b\right) - L_{y1}(a_1-a_2)\right]^3\left[2L_{x1}\left(4y_t - 3b - L_{y1}\right) + L_{y1}(a_1-a_2)\right]}{384{L_{x1}}^3{L_{y1}}^2}, \quad (74)$$

Preprints.org (www.preprints.org) | NOT PEER-REVIEWED | Posted: 24 January 2025 doi:10.20944/preprints202501.1740.v1

$$M_{yT} = \int_{y_t-\frac{L_{y1}(L_{x1}-a_1)}{L_{x1}}}^{y_t} \int_{-\frac{a_1}{2}}^{\frac{a_1}{2}} \sigma_z x dx dy + \int_{y_t-b}^{y_t-\frac{L_{y1}(L_{x1}-a_1)}{L_{x1}}} \int_{\frac{a_1}{2}+\frac{(y_t-L_{y1}-y)L_{x1}}{L_{y1}}}^{\frac{a_1}{2}} \sigma_z x dx dy + \int_{y_t-b-\frac{2L_{x1}(L_{y1}-b)-L_{y1}(a_1-a_2)}{2L_{x1}}}^{y_t-b} \int_{\frac{a_1}{2}+\frac{(y_t-L_{y1}-y)L_{x1}}{L_{y1}}}^{\frac{a_2}{2}} \sigma_z x dx dy, \quad (75)$$

$$M_{yT} = \frac{\sigma_{max}\left\{{a_1}^3{L_{y1}}^4(2L_{x1}-a_1) - {L_{x1}}^3\left(L_{y1}-b\right)^3\left[2L_{y1}a_1 - L_{x1}\left(L_{y1}-b\right)\right]\right\}}{24{L_{x1}}^2{L_{y1}}^3} + \frac{\sigma_{max}\left[2L_{x1}\left(L_{y1}-b\right) - L_{y1}(a_1-a_2)\right]^3\left[L_{y1}(a_1+3a_2) - 2L_{x1}\left(L_{y1}-b\right)\right]}{384{L_{x1}}^2{L_{y1}}^3}. \quad (76)$$

2.1.11. Case XI

$$R = \int_{y_t-b-\frac{2L_{x1}(L_{y1}-b)-L_{y1}(a_1+a_2)}{2L_{x1}}}^{y_t-b-\frac{2L_{x1}(L_{y1}-b)-L_{y1}(a_1-a_2)}{2L_{x1}}} \int_{\frac{a_1}{2}+\frac{(y_t-L_{y1}-y)L_{x1}}{L_{y1}}}^{\frac{a_2}{2}} \sigma_z dx dy + \int_{y_t-b-\frac{2L_{x1}(L_{y1}-b)-L_{y1}(a_1+a_2)}{2L_{x1}}}^{y_t-b} \int_{-\frac{a_2}{2}}^{\frac{a_2}{2}} \sigma_z dx dy + \int_{y_t-b}^{y_t-\frac{L_{y1}(L_{x1}-a_1)}{L_{x1}}} \int_{\frac{a_1}{2}+\frac{(y_t-L_{y1}-y)L_{x1}}{L_{y1}}}^{\frac{a_1}{2}} \sigma_z dx dy + \int_{y_t-\frac{L_{y1}(L_{x1}-a_1)}{L_{x1}}}^{y_t} \int_{-\frac{a_1}{2}}^{\frac{a_1}{2}} \sigma_z dx dy, \quad (77)$$

$$R = \frac{\sigma_{max}\left\{4\left[L_{y1}a_2 - L_{x1}\left(L_{y1}-b\right)\right]^3 + {L_{y1}}^3\left[4{L_{x1}}^3 - 4(L_{x1}-a_1)^3 + 3a_2({a_1}^2-{a_2}^2)\right]\right\}}{24{L_{x1}}^2{L_{y1}}^2} - \frac{\sigma_{max}a_2\left(L_{y1}-b\right)(a_1-a_2)}{2L_{x1}}, \quad (78)$$

Preprints.org (www.preprints.org) | NOT PEER-REVIEWED | Posted: 24 January 2025 doi:10.20944/preprints202501.1740.v1

$$M_{xT} = \int_{y_t-b-\frac{2L_{x1}(L_{y1}-b)-L_{y1}(a_1+a_2)}{2L_{x1}}}^{y_t-b-\frac{2L_{x1}(L_{y1}-b)-L_{y1}(a_1-a_2)}{2L_{x1}}} \int_{\frac{a_1}{2}+\frac{(y_t-L_{y1}-y)L_{x1}}{L_{y1}}}^{\frac{a_2}{2}} \sigma_z y dx dy + \int_{y_t-b-\frac{2L_{x1}(L_{y1}-b)-L_{y1}(a_1+a_2)}{2L_{x1}}}^{y_t-b} \int_{-\frac{a_2}{2}}^{\frac{a_2}{2}} \sigma_z y dx dy + \int_{y_t-b}^{y_t-\frac{L_{y1}(L_{x1}-a_1)}{L_{x1}}} \int_{\frac{a_1}{2}+\frac{(y_t-L_{y1}-y)L_{x1}}{L_{y1}}}^{\frac{a_1}{2}} \sigma_z y dx dy + \int_{y_t-\frac{L_{y1}(L_{x1}-a_1)}{L_{x1}}}^{y_t} \int_{-\frac{a_1}{2}}^{\frac{a_1}{2}} \sigma_z y dx dy, \quad (79)$$

$$M_{xT} = \frac{\sigma_{max}(4y_t-3b-L_{y1})\left\{4\left[L_{y1}a_2-L_{x1}(L_{y1}-b)\right]^3-3{L_{y1}}^2a_2(a_1-a_2)\left[4L_{x1}(L_{y1}-\right.\right.}{96{L_{x1}}^2{L_{y1}}^2} - \frac{\sigma_{max}a_2\left\{4\left[L_{x1}(L_{y1}-b)-L_{y1}a_1\right]^3-{L_{y1}}^2({a_1}^2-{a_2}^2)\left[3L_{x1}(L_{y1}-b)-2L_{y1}a_1\right]\right\}}{96{L_{x1}}^3L_{y1}} + \frac{\sigma_{max}L_{y1}\left[L_{y1}(L_{x1}-a_1)^4-4L_{x1}y_t(L_{x1}-a_1)^3+{L_{x1}}^4(4y_t-L_{y1})\right]}{24{L_{x1}}^3}, \quad (80)$$

$$M_{yT} = \int_{y_t-b-\frac{2L_{x1}(L_{y1}-b)-L_{y1}(a_1+a_2)}{2L_{x1}}}^{y_t-b-\frac{2L_{x1}(L_{y1}-b)-L_{y1}(a_1-a_2)}{2L_{x1}}} \int_{\frac{a_1}{2}+\frac{(y_t-L_{y1}-y)L_{x1}}{L_{y1}}}^{\frac{a_2}{2}} \sigma_z x dx dy + \int_{y_t-b-\frac{2L_{x1}(L_{y1}-b)-L_{y1}(a_1+a_2)}{2L_{x1}}}^{y_t-b} \int_{-\frac{a_2}{2}}^{\frac{a_2}{2}} \sigma_z x dx dy + \int_{y_t-b}^{y_t-\frac{L_{y1}(L_{x1}-a_1)}{L_{x1}}} \int_{\frac{a_1}{2}+\frac{(y_t-L_{y1}-y)L_{x1}}{L_{y1}}}^{\frac{a_1}{2}} \sigma_z x dx dy + \int_{y_t-\frac{L_{y1}(L_{x1}-a_1)}{L_{x1}}}^{y_t} \int_{-\frac{a_1}{2}}^{\frac{a_1}{2}} \sigma_z x dx dy, \quad (81)$$

$$M_{yT} = \frac{\sigma_{max}\left[{L_{x1}}^4(L_{y1}-b)^4-2a_1{L_{x1}}^3L_{y1}(L_{y1}-b)^3-2{a_2}^3L_{x1}{L_{y1}}^3b+{L_{y1}}^4({a_1}^3+{a_2}^3)\right.}{24{L_{x1}}^2{L_{y1}}^3} \quad (82)$$

2.1.12. Case XII

Preprints.org (www.preprints.org) | NOT PEER-REVIEWED | Posted: 24 January 2025 doi:10.20944/preprints202501.1740.v1

$$R = \int_{y_t-h_y}^{y_t-b-\frac{2L_{x1}(L_{y1}-b)-L_{y1}(a_1+a_2)}{2L_{x1}}} \int_{\frac{a_1}{2}+\frac{(y_t-L_{y1}-y)L_{x1}}{L_{y1}}}^{\frac{a_2}{2}} \sigma_z dxdy + \int_{y_t-b-\frac{2L_{x1}(L_{y1}-b)-L_{y1}(a_1+a_2)}{2L_{x1}}}^{y_t-b} \int_{-\frac{a_2}{2}}^{\frac{a_2}{2}} \sigma_z dxdy + \int_{y_t-b}^{y_t-\frac{L_{y1}(L_{x1}-a_1)}{L_{x1}}} \int_{\frac{a_1}{2}+\frac{(y_t-L_{y1}-y)L_{x1}}{L_{y1}}}^{\frac{a_2}{2}} \sigma_z dxdy + \int_{y_t-\frac{L_{y1}(L_{x1}-a_1)}{L_{x1}}}^{y_t} \int_{-\frac{a_1}{2}}^{\frac{a_1}{2}} \sigma_z dxdy, \quad (83)$$

$$R = \frac{\sigma_{max}\{(a_1+a_2)^2[L_{y1}(a_1+a_2)-6L_{x1}(L_{y1}-h_y)]-24L_{x1}a_1a_2(h_y-b)\}}{48{L_{x1}}^2} + \frac{\sigma_{max}\{6L_{y1}a_2(L_{y1}-b)^2-(L_{y1}-h_y)^2[2L_{x1}(L_{y1}-h_y)-3L_{y1}(a_1-a_2)]\}}{12{L_{y1}}^2}, \quad (84)$$

$$M_{xT} = \int_{y_t-h_y}^{y_t-b-\frac{2L_{x1}(L_{y1}-b)-L_{y1}(a_1+a_2)}{2L_{x1}}} \int_{\frac{a_1}{2}+\frac{(y_t-L_{y1}-y)L_{x1}}{L_{y1}}}^{\frac{a_2}{2}} \sigma_z y dxdy + \int_{y_t-b-\frac{2L_{x1}(L_{y1}-b)-L_{y1}(a_1+a_2)}{2L_{x1}}}^{y_t-b} \int_{-\frac{a_2}{2}}^{\frac{a_2}{2}} \sigma_z y dxdy + \int_{y_t-b}^{y_t-\frac{L_{y1}(L_{x1}-a_1)}{L_{x1}}} \int_{\frac{a_1}{2}+\frac{(y_t-L_{y1}-y)L_{x1}}{L_{y1}}}^{\frac{a_2}{2}} \sigma_z y dxdy + \int_{y_t-\frac{L_{y1}(L_{x1}-a_1)}{L_{x1}}}^{y_t} \int_{-\frac{a_1}{2}}^{\frac{a_1}{2}} \sigma_z y dxdy, \quad (85)$$

$$M_{xT} = \frac{\sigma_{max}L_{y1}\{(4y_t-L_{y1}){L_{x1}}^4-(L_{x1}-a_1)^3[L_{x1}(4y_t-L_{y1})+L_{y1}a_1]\}}{24{L_{x1}}^3} - \frac{\sigma_{max}L_{x1}(L_{y1}-b)^3(4y_t-3b-L_{y1})}{24{L_{y1}}^2} + \frac{\sigma_{max}[2L_{x1}(L_{y1}-b)-L_{y1}(a_1-a_2)]^3[2L_{x1}(4y_t-3b)-L_{y1}(2L_{x1}-a_1+a_2)]}{384{L_{x1}}^3{L_{y1}}^2} - \frac{\sigma_{max}[2L_{x1}(L_{y1}-b)-L_{y1}(a_1+a_2)]^3[2L_{x1}(4y_t-3b)-L_{y1}(2L_{x1}-a_1-a_2)]}{384{L_{x1}}^3{L_{y1}}^2} - \frac{\sigma_{max}[2L_{x1}(L_{y1}-h_y)-L_{y1}(a_1-a_2)]^3[2L_{x1}(4y_t-3h_y)-L_{y1}(2L_{x1}-a_1+a_2)]}{384{L_{x1}}^3{L_{y1}}^2}, \quad (86)$$

Preprints.org (www.preprints.org) | NOT PEER-REVIEWED | Posted: 24 January 2025 doi:10.20944/preprints202501.1740.v1

$$M_{yT} = \int_{y_t-h_y}^{y_t-b-\frac{2L_{x1}(L_{y1}-b)-L_{y1}(a_1+a_2)}{2L_{x1}}} \int_{\frac{a_1}{2}+\frac{(y_t-L_{y1}-y)L_{x1}}{L_{y1}}}^{\frac{a_2}{2}} \sigma_z x dx dy + \int_{y_t-b-\frac{2L_{x1}(L_{y1}-b)-L_{y1}(a_1+a_2)}{2L_{x1}}}^{y_t-b} \int_{-\frac{a_2}{2}}^{\frac{a_2}{2}} \sigma_z x dx dy + \int_{y_t-b}^{y_t-\frac{L_{y1}(L_{x1}-a_1)}{L_{x1}}} \int_{\frac{a_1}{2}+\frac{(y_t-L_{y1}-y)L_{x1}}{L_{y1}}}^{\frac{a_1}{2}} \sigma_z x dx dy + \int_{y_t-\frac{L_{y1}(L_{x1}-a_1)}{L_{x1}}}^{y_t} \int_{-\frac{a_1}{2}}^{\frac{a_1}{2}} \sigma_z x dx dy, \quad (87)$$

$$M_{yT} = \frac{\sigma_{max}\left[{L_{x1}}^4(L_{y1}-b)^4 - 2a_1{L_{x1}}^3L_{y1}(L_{y1}-b)^3 - 2{a_2}^3L_{x1}{L_{y1}}^3b + {L_{y1}}^4({a_1}^3+{a_2}^3)\right.}{24{L_{x1}}^2{L_{y1}}^3} + \frac{\sigma_{max}\left[2L_{x1}(L_{y1}-h_y)-L_{y1}(a_1-a_2)\right]^3\left[L_{y1}(a_1+3a_2)-2L_{x1}(L_{y1}-h_y)\right]}{384{L_{x1}}^2{L_{y1}}^3}. \quad (88)$$

2.1.13. Case XIII

$$R = \int_{y_t-\frac{L_{y1}(L_{x1}-a_1)}{L_{x1}}}^{y_t} \int_{-\frac{a_1}{2}}^{\frac{a_1}{2}} \sigma_z dx dy + \int_{y_t-b}^{y_t-\frac{L_{y1}(L_{x1}-a_1)}{L_{x1}}} \int_{\frac{a_1}{2}+\frac{(y_t-y)L_{x1}}{L_{y1}}-L_{x1}}^{\frac{a_1}{2}} \sigma_z dx dy + \int_{y_t-hy}^{y_t-b} \int_{-\frac{a_2}{2}}^{\frac{a_2}{2}} \sigma_z dx dy, \quad (89)$$

$$R = \frac{\sigma_{max}\left\{3a_2{L_{x1}}^2L_{y1}\left[(L_{y1}-b)^2-(L_{y1}-h_y)^2\right]-{L_{y1}}^3(L_{x1}-a_1)^3\right\}}{6{L_{x1}}^2{L_{y1}}^2} + \frac{\sigma_{max}\left\{{L_{x1}}^3\left[{L_{y1}}^3-(L_{y1}-b)^3\right]-3a_1a_2L_{x1}{L_{y1}}^2(h_y-b)\right\}}{6{L_{x1}}^2{L_{y1}}^2}, \quad (90)$$

$$M_{xT} = \int_{y_t-\frac{L_{y1}(L_{x1}-a_1)}{L_{x1}}}^{y_t} \int_{-\frac{a_1}{2}}^{\frac{a_1}{2}} \sigma_z y dx dy + \int_{y_t-b}^{y_t-\frac{L_{y1}(L_{x1}-a_1)}{L_{x1}}} \int_{\frac{a_1}{2}+\frac{(y_t-y)L_{x1}}{L_{y1}}-L_{x1}}^{\frac{a_1}{2}} \sigma_z y dx dy + \int_{y_t-hy}^{y_t-b} \int_{-\frac{a_2}{2}}^{\frac{a_2}{2}} \sigma_z y dx dy, \quad (91)$$

Preprints.org (www.preprints.org) | NOT PEER-REVIEWED | Posted: 24 January 2025 doi:10.20944/preprints202501.1740.v1

$$M_{xT} = \frac{\sigma_{max}\{a_2 {h_y}^2[2h_y - 3(L_{y1} + y_t)] + b^2[2b(L_{x1} - a_2) + 3a_2(L_{y1} + y_t)]\}}{6L_{y1}} + \frac{\sigma_{max}(L_{x1} - a_1)^3[L_{y1}(L_{x1} - a_1) - 4L_{x1}y_t]}{24{L_{y1}}^2} + \frac{\sigma_{max}a_2(b - h_y)[2y_t(a_1 - 2L_{x1}) - a_1(b + h_y)]}{4L_{x1}} + \frac{\sigma_{max}L_{x1}\left[2{L_{y1}}^2(2L_{y1}y_t - 3b^2) - 3b^4 - 4y_t(L_{y1} - b)^3\right]}{24{L_{y1}}^2}, \quad (92)$$

$$M_{yT} = \int_{y_t - \frac{L_{y1}(L_{x1} - a_1)}{L_{x1}}}^{y_t} \int_{-\frac{a_1}{2}}^{\frac{a_1}{2}} \sigma_z x dx dy + \int_{y_t - b}^{y_t - \frac{L_{y1}(L_{x1} - a_1)}{L_{x1}}} \int_{\frac{a_1}{2} + \frac{(y_t - y)L_{x1}}{L_{y1}} - L_{x1}}^{\frac{a_1}{2}} \sigma_z x dx dy + \int_{y_t - hy}^{y_t - b} \int_{-\frac{a_2}{2}}^{\frac{a_2}{2}} \sigma_z x dx dy, \quad (93)$$

$$M_{yT} = \frac{\sigma_{max}\left\{{L_{x1}}^3(L_{y1} - b)^3[L_{x1}(L_{y1} - b) - 2a_1L_{y1}] + {L_{y1}}^3[{a_1}^3L_{y1}(2L_{x1} - a_1) + 2{a_2}^3L\right.}{24{L_{x1}}^2{L_{y1}}^3} \quad (94)$$

2.1.14. Case XIV

$$R = \int_{y_t - b}^{y_t} \int_{-\frac{a_1}{2}}^{\frac{a_1}{2}} \sigma_z dx dy + \int_{y_t - b - \frac{2L_{x1}(L_{y1} - b) - L_{y1}(a_1 + a_2)}{2L_{x1}}}^{y_t - b} \int_{-\frac{a_2}{2}}^{\frac{a_2}{2}} \sigma_z dx dy + \int_{y_t - b - \frac{2L_{x1}(L_{y1} - b) - L_{y1}(a_1 - a_2)}{2L_{x1}}}^{y_t - b - \frac{2L_{x1}(L_{y1} - b) - L_{y1}(a_1 + a_2)}{2L_{x1}}} \int_{\frac{a_1}{2} + \frac{(y_t - y)L_{x1}}{L_{y1}} - L_{x1}}^{\frac{a_2}{2}} \sigma_z dx dy, \quad (95)$$

$$R = \frac{\sigma_{max}\{{L_{y1}}^2{a_2}^3 + 3{L_{y1}}^2a_2(2L_{x1} - a_1)^2 - 12L_{x1}b(a_1 - a_2)[L_{y1}(a_1 - 2L_{x1}) + L_{x1}l}{24{L_{x1}}^2L_{y1}} \quad (96)$$

$$M_{xT} = \int_{y_t - b}^{y_t} \int_{-\frac{a_1}{2}}^{\frac{a_1}{2}} \sigma_z y dx dy + \int_{y_t - b - \frac{2L_{x1}(L_{y1} - b) - L_{y1}(a_1 + a_2)}{2L_{x1}}}^{y_t - b} \int_{-\frac{a_2}{2}}^{\frac{a_2}{2}} \sigma_z y dx dy + \int_{y_t - b - \frac{2L_{x1}(L_{y1} - b) - L_{y1}(a_1 - a_2)}{2L_{x1}}}^{y_t - b - \frac{2L_{x1}(L_{y1} - b) - L_{y1}(a_1 + a_2)}{2L_{x1}}} \int_{\frac{a_1}{2} + \frac{(y_t - y)L_{x1}}{L_{y1}} - L_{x1}}^{\frac{a_2}{2}} \sigma_z y dx dy, \quad (97)$$

Preprints.org (www.preprints.org) | NOT PEER-REVIEWED | Posted: 24 January 2025 doi:10.20944/preprints202501.1740.v1

$$M_{xT} = \frac{\sigma_{max}\left\{a_2{L_{y1}}^3[a_1{a_2}^2 - (2L_{x1} - a_1)^3] - 24{L_{x1}}^3 y_t(a_1 - a_2)\left(L_{y1} - b\right)^2\right\}}{48{L_{x1}}^3 L_{y1}} - \frac{\sigma_{max}\{b(a_1 - a_2)[3L_{y1}a_1(2y_t - b) + 2L_{x1}b(3L_{y1} - 2b)]\}}{12L_{x1}L_{y1}} + \frac{\sigma_{max}L_{y1}\{3a_1y_t[a_1a_2 + 4L_{x1}(L_{x1} - a_2)] - {a_2}^3(L_{y1} - y_t)\}}{24{L_{x1}}^2}, \quad (98)$$

$$M_{yT} = \int_{y_t-b}^{y_t}\int_{-\frac{a_1}{2}}^{\frac{a_1}{2}}\sigma_z x dxdy + \int_{y_t-b}^{y_t-b-\frac{2L_{x1}(L_{y1}-b)-L_{y1}(a_1+a_2)}{2L_{x1}}}\int_{-\frac{a_2}{2}}^{\frac{a_2}{2}}\sigma_z x dxdy + \int_{y_t-b-\frac{2L_{x1}(L_{y1}-b)-L_{y1}(a_1+a_2)}{2L_{x1}}}^{y_t-b-\frac{2L_{x1}(L_{y1}-b)-L_{y1}(a_1-a_2)}{2L_{x1}}}\int_{\frac{a_1}{2}+\frac{(y_t-y)L_{x1}}{L_{y1}}-L_{x1}}^{\frac{a_2}{2}}\sigma_z x dxdy, \quad (99)$$

$$M_{yT} = \frac{\sigma_{max}\{2L_{x1}[{a_1}^3 b + {a_2}^3(L_{y1} - b)] - L_{y1}a_1{a_2}^3\}}{24{L_{x1}}^2}. \quad (100)$$

2.1.15. Case XV

$$R = \int_{y_t-b}^{y_t}\int_{-\frac{a_1}{2}}^{\frac{a_1}{2}}\sigma_z dxdy + \int_{y_t-b}^{y_t-b-\frac{2L_{x1}(L_{y1}-b)-L_{y1}(a_1+a_2)}{2L_{x1}}}\int_{-\frac{a_2}{2}}^{\frac{a_2}{2}}\sigma_z dxdy + \int_{y_t-h_y}^{y_t-b-\frac{2L_{x1}(L_{y1}-b)-L_{y1}(a_1+a_2)}{2L_{x1}}}\int_{\frac{a_1}{2}+\frac{(y_t-y)L_{x1}}{L_{y1}}-L_{x1}}^{\frac{a_2}{2}}\sigma_z dxdy, \quad (101)$$

$$R = \frac{\sigma_{max}\left\{2L_{x1}\left[{L_{y1}}^3 - \left(L_{y1} - h_y\right)^3\right] - 3L_{y1}(a_1 - a_2)\left[2\left(L_{y1} - b\right)^2 - \left(L_{y1} - h_y\right)^2\right]\right\}}{12{L_{y1}}^2} - \frac{\sigma_{max}\{6L_{x1}(a_1 - a_2)[4a_1b - h_y(a_1 - a_2)] + L_{y1}[(L_{x1} - a_1 - a_2)^3 - 12{L_{x1}}^2(a_1 -}{48{L_{x1}}^2} \quad (102)$$

$$M_{xT} = \int_{y_t-b}^{y_t}\int_{-\frac{a_1}{2}}^{\frac{a_1}{2}}\sigma_z y dxdy + \int_{y_t-b}^{y_t-b-\frac{2L_{x1}(L_{y1}-b)-L_{y1}(a_1+a_2)}{2L_{x1}}}\int_{-\frac{a_2}{2}}^{\frac{a_2}{2}}\sigma_z y dxdy + \int_{y_t-h_y}^{y_t-b-\frac{2L_{x1}(L_{y1}-b)-L_{y1}(a_1+a_2)}{2L_{x1}}}\int_{\frac{a_1}{2}+\frac{(y_t-y)L_{x1}}{L_{y1}}-L_{x1}}^{\frac{a_2}{2}}\sigma_z y dxdy, \quad (103)$$

Preprints.org (www.preprints.org) | NOT PEER-REVIEWED | Posted: 24 January 2025 doi:10.20944/preprints202501.1740.v1

$$M_{xT} = \frac{\sigma_{max}\left\{\left[L_{x1}(L_{y1}-b)-L_{y1}a_1\right]^3\left[L_{x1}(4y_t-3b)-L_{y1}(L_{x1}-a_1)\right]-{L_{y1}}^3(L_{x1}-a_1)\right.}{24{L_{x1}}^3{L_{y1}}^2}$$
$$+\frac{\sigma_{max}\left[L_{x1}{L_{y1}}^3(4y_t-L_{y1})-L_{x1}(L_{y1}-b)^3(4y_t-3b-L_{y1})\right]}{24{L_{y1}}^2}$$
$$+\frac{\sigma_{max}\left[2L_{x1}(L_{y1}-b)-L_{y1}(a_1-a_2)\right]^3\left[2L_{x1}(4y_t-3b)-L_{y1}(2L_{x1}-a_1+a_2)\right]}{384{L_{x1}}^3{L_{y1}}^2} \quad (104)$$
$$-\frac{\sigma_{max}\left[2L_{x1}(L_{y1}-b)-L_{y1}(a_1+a_2)\right]^3\left[2L_{x1}(4y_t-3b)-L_{y1}(2L_{x1}-a_1-a_2)\right]}{384{L_{x1}}^3{L_{y1}}^2}$$
$$-\frac{\sigma_{max}\left[2L_{x1}(L_{y1}-h_y)-L_{y1}(a_1-a_2)\right]^3\left[2L_{x1}(4y_t-3h_y)-L_{y1}(2L_{x1}-a_1+a_2)\right]}{384{L_{x1}}^3{L_{y1}}^2},$$

$$M_{yT} = \int_{y_t-b}^{y_t}\int_{-\frac{a_1}{2}}^{\frac{a_1}{2}}\sigma_z x\,dx\,dy + \int_{y_t-b}^{y_t-b-\frac{2L_{x1}(L_{y1}-b)-L_{y1}(a_1+a_2)}{2L_{x1}}}\int_{-\frac{a_2}{2}}^{\frac{a_2}{2}}\sigma_z x\,dx\,dy \quad (105)$$
$$+\int_{y_t-h_y}^{y_t-b-\frac{2L_{x1}(L_{y1}-b)-L_{y1}(a_1+a_2)}{2L_{x1}}}\int_{\frac{a_1}{2}+\frac{(y_t-y)L_{x1}}{L_{y1}}-L_{x1}}^{\frac{a_2}{2}}\sigma_z x\,dx\,dy,$$

$$M_{yT} = \frac{\sigma_{max}\left\{16{a_1}^3{L_{x1}}^2L_{y1}(2L_{x1}-a_1)+\left[2L_{x1}(L_{y1}-b)-L_{y1}(a_1-a_2)\right]^3\left[L_{y1}(a_1+3a_2\right.\right.}{384{L_{x1}}^2{L_{y1}}^3}$$
$$-\frac{\sigma_{max}\left\{{L_{x1}}^3(L_{y1}-b)^3\left[2L_{y1}a_1-L_{x1}(L_{y1}-b)\right]+\left[L_{x1}(L_{y1}-b)-L_{y1}a_1\right]^3\left[L_{y1}a_1+\right.\right.}{24{L_{x1}}^2{L_{y1}}^3} \quad (106)$$
$$-\frac{\sigma_{max}\left[2L_{x1}(L_{y1}-b)-L_{y1}(a_1+a_2)\right]^3\left[L_{y1}(a_1-3a_2)-2L_{x1}(L_{y1}-b)\right]}{384{L_{x1}}^2{L_{y1}}^3}$$
$$-\frac{\sigma_{max}\left[2L_{x1}(L_{y1}-h_y)-L_{y1}(a_1-a_2)\right]^3\left[L_{y1}(a_1+3a_2)-2L_{x1}(L_{y1}-h_y)\right]}{384{L_{x1}}^2{L_{y1}}^3}.$$

2.2. Special Cases

There are two cases: Case X) when the moments M_{x1} and M_{x2} are zero; Case Y) when moments M_{y1} and M_{y2} are zero.

2.2.1. Case Y

Figure 5 shows the three possible cases for a T-shaped combined footing subjected to axial load and a bending moment around the X axis provided by each column (M_{y1} and M_{y2} are zero).

For case Y-I, it is assumed that the entire bottom surface of the footing works under compression, and equations (15) to (22) are used.

For cases Y-IIA and Y-IIB, it is assumed that the entire bottom surface of the footing works partially under compression

The pressures generated by the ground on the footing are obtained by means of the general equation of the pressure plane, starting from three known points.

Now, the three known points of the pressure plane are:

Preprints.org (www.preprints.org) | NOT PEER-REVIEWED | Posted: 24 January 2025 doi:10.20944/preprints202501.1740.v1

$$p_1\left(\frac{a_1}{2}, y_t, \sigma_{max}\right);\ p_2\left(-\frac{a_1}{2}, y_t, \sigma_{max}\right);\ p_3\left(\frac{a_2}{2}, y_t - L_{y1}, 0\right). \tag{107}$$

The general equation of the pressure plane is obtained as follows:

$$\begin{vmatrix} x - \frac{a_1}{2} & y - y_t & \sigma_z - \sigma_{max} \\ -a_1 & 0 & 0 \\ \frac{a_2 - a_1}{2} & -L_{y1} & -\sigma_{max} \end{vmatrix}. \tag{108}$$

Solving the determinant of equation (108) gives the pressure at any point "σ_z":

$$\sigma_z = \frac{\sigma_{max}(L_{y1} - y_t + y)}{L_{y1}}. \tag{109}$$

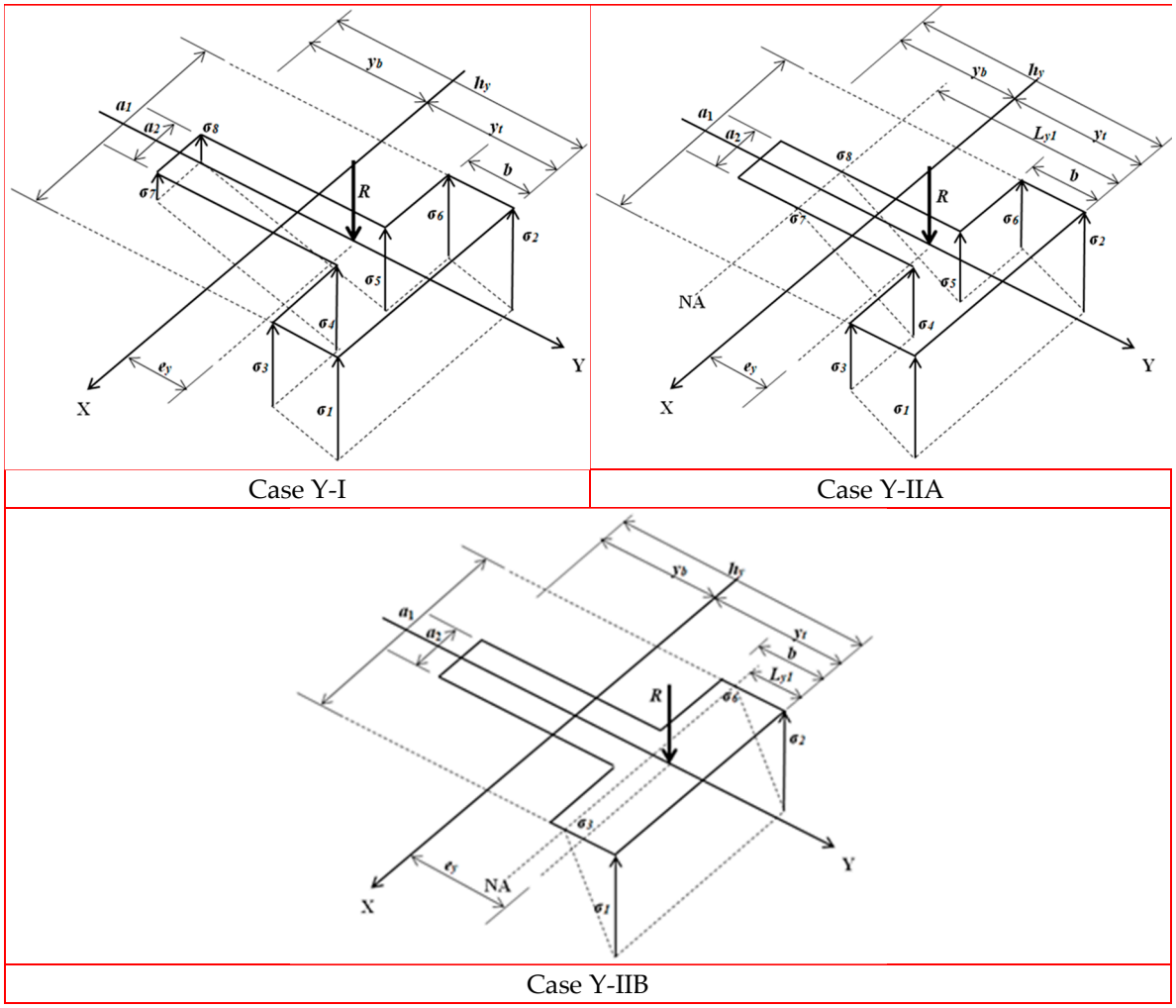

Figure 5. Case Y for T-shaped combined footings.

2.2.1.1. Case Y-IIA

The general equations for R and M_{xT} are:

$$R = 2\int_{y_t-b}^{y_t}\int_{0}^{\frac{a_1}{2}} \sigma_z dxdy + 2\int_{y_t-L_{y1}}^{y_t-b}\int_{0}^{\frac{a_2}{2}} \sigma_z dxdy, \tag{110}$$

Preprints.org (www.preprints.org) | NOT PEER-REVIEWED | Posted: 24 January 2025 doi:10.20944/preprints202501.1740.v1

$$R = \frac{\sigma_{max}\left[a_1 b\left(2L_{y1} - b\right) + a_2\left(L_{y1} - b\right)^2\right]}{2L_{y1}}, \tag{111}$$

$$M_{xT} = 2\int_{y_t-b}^{y_t}\int_0^{\frac{a_1}{2}} \sigma_z y dx dy + 2\int_{y_t-L_{y1}}^{y_t-b}\int_0^{\frac{a_2}{2}} \sigma_z y dx dy, \tag{112}$$

$$M_{xT} = \frac{\sigma_{max} b(a_1 - a_2)\left[2b^2 + 6L_{y1}y_t - 3b\left(L_{y1} + y_t\right)\right]}{6L_{y1}} + \frac{\sigma_{max}\left\{a_2 {L_{y1}}^2\left(3y_t - L_{y1}\right)\right\}}{6L_{y1}}. \tag{113}$$

2.2.1.2. Case Y-IIB

The general equations for R and M_{xT} are:

$$R = 2\int_{y_t-L_{y1}}^{y_t}\int_0^{\frac{a_1}{2}} \sigma_z dx dy, \tag{114}$$

$$R = \frac{\sigma_{max} a_1 L_{y1}}{2}, \tag{115}$$

$$M_{xT} = 2\int_{y_t-L_{y1}}^{y_t}\int_0^{\frac{a_1}{2}} \sigma_z y dx dy, \tag{116}$$

$$M_{xT} = \frac{\sigma_{max} a_1 L_{y1}\left(3y_t - L_{y1}\right)}{6}. \tag{117}$$

2.2.2. Case X

For the T-shaped combined footing subjected to axial load and a bending moment around the Y axis provided by each column (M_{x1} and M_{x2} are zero).

For the case X, all the equations of the biaxial bending must be used, because there are resultant moments M_{xT}.

2.3. Minimum Surface for T-Shaped Combined Footings

Minimum surface (objective function) for all cases is:

$$A_{min} = (a_1 - a_2)b + a_2 h_y. \tag{118}$$

Table 1 shows the equations of the constraint functions for biaxial bending in each case.

Table 1. Constraint functions for biaxial bending.

Case	Equations
I	Equations (1) to (5), (7) to (9), (15) to (22), $0 \leq \sigma_1$ to $\sigma_8 \leq \sigma_{max}$
II	Equations (1), (2), (7) to (9), (24), (26), (28), $L_{y1} \leq b$, $L_{x1} \leq a_1$
III	Equations (1), (2), (7) to (9), (30), (32), (34), $L_{y1} \geq b$, $L_{x1} \leq a_1$
IV	Equations (1), (2), (7) to (9), (36), (38), (40), $L_{y1} \geq b$, $L_{x1} \leq a_1$
V	Equations (1), (2), (7) to (9), (42), (44), (46), $L_{y1} \geq h_y$, $L_{x1} \leq a_1$
VI	Equations (1), (2), (7) to (9), (48), (50), (52), $L_{y1} \geq h_y$, $L_{x1} \leq a_1$

Preprints.org (www.preprints.org) | NOT PEER-REVIEWED | Posted: 24 January 2025 doi:10.20944/preprints202501.1740.v1

VII	Equations (1), (2), (7) to (9), (54), (56), (58), $L_{y1} \geq h_y$, $L_{x1} \leq a_1$
VIII	Equations (1), (2), (7) to (9), (60), (62), (64), $L_{y1} \leq b$, $L_{x1} \geq a_1$
IX	Equations (1), (2), (7) to (9), (66), (68), (70), $L_{y1} \geq b$, $L_{x1} \geq a_1$
X	Equations (1), (2), (7) to (9), (72), (74), (76), $L_{y1} \geq b$, $L_{x1} \geq a_1$
XI	Equations (1), (2), (7) to (9), (78), (80), (82), $L_{y1} \geq b$, $L_{x1} \geq a_1$
XII	Equations (1), (2), (7) to (9), (84), (86), (88), $L_{y1} \geq b$, $L_{x1} \geq a_1$
XIII	Equations (1), (2), (7) to (9), (90), (92), (94), $L_{y1} \geq b$, $L_{x1} \geq a_1$
XIV	Equations (1), (2), (7) to (9), (96), (98), (100), $L_{y1} \geq b$, $L_{x1} \geq a_1$
XV	Equations (1), (2), (7) to (9), (102), (104), (106), $L_{y1} \geq b$, $L_{x1} \geq a_1$

Note: all cases must include $h_y = L_1 + L + L_2$, $h_y \geq b$, $L_1 \leq b/2$, $a_2 \leq a_1$.

The functions that must be limited in the Y-axis direction are:
Not limited: $L_1 \geq c_1/2$ and $L_2 \geq c_3/2$.
Limited in column 1: $L_1 = c_1/2$ and $L_2 \geq c_3/2$.
Limited in column 2: $L_1 \geq c_1/2$ and $L_2 = c_3/2$.
Limited in the two columns: $L_1 = c_1/2$ and $L_2 = c_3/2$.
Note: c_1 and c_3 are the sides of the columns in the Y direction.
Table 2 shows the equations of the constraint functions for uniaxial bending in each case (Case Y).

Table 2. Constraint functions for uniaxial bending.

Case	Equations
Y-I	Equations (1) to (5), (7) to (9), (15) to (22), $0 \leq \sigma_1$ to $\sigma_8 \leq \sigma_{max}$
Y-IIA	Equations (1), (2), (7) to (9), (111) to (113), $L_{y1} \geq b$, $L_{y1} \leq h_y$
Y-IIB	Equations (1), (2), (7) to (9), (115) to (117), $L_{y1} \leq b$

Note: all cases must include $h_y = L_1 + L + L_2$, $h_y \geq b$, $L_1 \leq b/2$, $a_2 \leq a_1$.

3. Numerical Examples

Three numerical examples are shown for T-shaped combined footings supporting two columns, and each example presents four types of constraints, the constraints are: Constraint 1 is for unconstrained sides ($L_1 \geq c_1/2$ and $L_2 \geq c_3/2$); Constraint 2 is for a side constrained in column 1 ($L_1 = c_1/2$ and $L_2 \geq c_3/2$); Constraint 3 is for a side constrained in column 2 ($L_1 \geq c_1/2$ and $L_2 = c_3/2$); Constraint 4 is for two sides constrained (opposite sides) ($L_1 = c_1/2$ and $L_2 = c_3/2$). Example 1 is for a T-shaped combined footing subjected to axial load and moments on the X and Y axes due to the columns. Example 2 is for a T-shaped combined footing subjected to axial load and a moment on the Y axis due to the columns. Example 3 is for a T-shaped combined footing subjected to axial load and a moment on the X axis due to the columns.

The data for example 1 are: $c_1 = 0.40$ *m*, $c_3 = 0.40$ *m*, $P_1 = 1250$ *kN*, $P_2 = 250$ *kN*, $M_{x1} = 300$ *kN-m*, $M_{x2} = 150$ *kN-m*, $M_{y1} = 200$ *kN-m*, $M_{y2} = 200$ *kN-m*, $L = 6.00$ *m*, $\sigma_{max} = 200$ *kN/m²*. The data for example 2 are: the same as for example 1, but $M_{x1} = 0$ *kN-m*, $M_{x2} = 0$ *kN-m*. The data for example 3 are: the same as for example 1, but $M_{y1} = 0$ *kN-m*, $M_{y2} = 0$ *kN-m*.

Table 3 shows the results of the example 1.
Table 4 shows the results of the example 2.
Table 5 shows the results of the example 3.

Table 3. Example 1.

Case	A_{min} m^2			
	Ends not limited	Limited at L_1	Limited at L_2	Limited at L_1 and L_2
I	13.11	17.10	13.11	17.10

Preprints.org (www.preprints.org) | NOT PEER-REVIEWED | Posted: 24 January 2025 doi:10.20944/preprints202501.1740.v1

II	45.00	*	*	*
III	15.85	*	15.85	*
IV	21.93	*	*	*
V	15.62	*	15.62	*
VI	11.59	11.73	11.59	15.51
VII	15.53	*	15.53	*
VIII	23.45	22.36	23.45	22.36
IX	12.61	16.78	12.61	16.78
X	14.09	14.46	14.09	14.46
XI	12.98	16.58	12.98	16.58
XII	14.94	*	14.94	*
XIII	12.88	16.46	12.88	16.46
XIV	13.12	13.44	13.12	13.44
XV	12.71	*	12.71	*

Note: * No solution available.

Table 4. Example 2.

Case	A_{min} m^2			
	Ends not limited	**Limited at L_1**	**Limited at L_2**	**Limited at L_1 and L_2**
I	12.57	12.80	12.57	12.80
II	45.00	*	*	*
III	15.55	*	15.53	*
IV	21.91	*	*	*
V	15.26	*	15.26	*
VI	15.37	12.25	12.90	12.90
VII	15.06	*	15.05	*
VIII	22.45	22.45	22.45	22.45
IX	12.56	15.82	12.56	15.82
X	13.61	13.79	13.61	13.79
XI	15.66	15.48	10.40	15.48
XII	13.15	*	13.51	*
XIII	12.56	15.45	12.56	15.45
XIV	12.68	12.82	12.68	12.82
XV	11.88	12.78	11.14	12.16

Note: * No solution available.

Table 5. Example 3.

Case	A_{min} m^2			
	Ends not limited	**Limited at L_1**	**Limited at L_2**	**Limited at L_1 and L_2**
YI	11.50	16.74	11.50	16.74
YIIA	11.34	11.87	11.34	11.87
YIIB	15.00	18.70	15.00	18.70

Preprints.org (www.preprints.org) | NOT PEER-REVIEWED | Posted: 24 January 2025 doi:10.20944/preprints202501.1740.v1

4. Results

The results of the table 3 show the following:

1.- The value of "A_{min}" is the same for constraint 1 and 3, except in cases II and IV that there is no solution available in constraint 3.

2.- The value of "A_{min}" is the same for constraint 2 and 4, except in case VI that there is solution available, but it is different.

3.- The minimum areas "A_{min}" are presented in case VI for constraints 1, 2 and 3, and case XIV for constraint 4.

The results of the table 4 show the following:

1.- The value of "A_{min}" is the same for constraint 1 and 3, except in cases II and IV that there is no solution available in constraint 3, and also for cases III, VI, VII, XI XII, XV these are different.

2.- The value of "A_{min}" is the same for constraint 2 and 4, except in cases VI and XV that there is solution available, but these are different.

3.- The minimum areas "A_{min}" are presented in case XV for constraint 1, in case VI for constraint 2, in case XI for constraint 3 and in case XV for constraint 4.

The results of the table 5 show the following:

1.- The value of "A_{min}" is the same for constraint 1 and 3.

2.- The value of "A_{min}" is the same for constraint 2 and 4.

3.- The minimum areas "A_{min}" are presented in case YIIA for all the constraints.

Tables 6 to 8 show in detail the mechanical and geometric properties of the cases that present the minimum areas of each example.

Table 6. Mechanical and geometric properties of the cases that present the minimum areas of the example 1.

Case	R kN	M_{xT} kN-m	M_{yT} kN-m	L_1 m	L_2 m	L_{x1} m	L_{y1} m	a_1 m	a_2 m	b m	h_y m	y_t m	A_{min} m^2
Ends not limited													
VI	1500	2034.12	400	0.20	0.20	0.92	6.40	3.38	1.00	2.18	6.40	2.26	11.59
Limited footing at L_1													
VI	1500	2663.63	400	0.20	1.19	0.92	7.39	3.32	1.00	1.87	7.39	2.68	11.73
Limited footing at L_2													
VI	1500	2034.12	400	0.20	0.20	0.92	6.40	3.38	1.00	2.18	6.40	2.26	11.59
Limited footing at L_1 and L_2													
XIV	1500	1328.82	400	0.20	0.20	21.83	6.83	8.04	1.00	1.00	6.40	1.79	13.44

Table 7. Mechanical and geometric properties of the cases that present the minimum areas of the example 2.

Case	R kN	M_{xT} kN-m	M_{yT} kN-m	L_1 m	L_2 m	L_{x1} m	L_{y1} m	a_1 m	a_2 m	b m	h_y m	y_t m	A_{min} m^2
Ends not limited													
XV	1500	1095.78	400	0.25	0.20	50.00	5.54	6.44	1.00	1.00	6.45	1.98	11.88
Limited footing at L_1													
VI	1500	4437.68	400	0.20	3.78	0.92	9.98	3.27	1.00	1.00	9.98	4.16	12.25
Limited footing at L_2													
XI	1500	0	400	4.20	0.20	8.40	20.05	1.00	1.00	10.40	10.40	5.20	10.40
Limited footing at L_1 and L_2													

Preprints.org (www.preprints.org) | NOT PEER-REVIEWED | Posted: 24 January 2025 doi:10.20944/preprints202501.1740.v1

XV	1500	1081.82	400	0.20	0.20	38.73	5.50	6.76	1.00	1.00	6.40	1.92	12.16

Table 8. Mechanical and geometric properties of the cases that present the minimum areas of the example 3.

Case	R kN	M_{xT} kN-m	M_{yT} kN-m	L_1 m	L_2 m	L_{y1} m	a_1 m	a_2 m	b m	h_y m	y_t m	A_{min} m^2
Ends not limited												
YIIA	1500	1476.28	0	0.50	0.20	6.44	5.64	1.00	1.00	6.70	2.18	11.34
Limited footing at L_1												
YIIA	1500	1582.81	0	0.20	0.20	5.12	6.47	1.00	1.00	6.40	1.96	11.87
Limited footing at L_2												
YIIA	1500	1476.28	0	0.50	0.20	6.44	5.64	1.00	1.00	6.70	2.18	11.34
Limited footing at L_1 and L_2												
YIIA	1500	1582.81	0	0.20	0.20	5.12	6.47	1.00	1.00	6.40	1.96	11.87

The results of the table 6 show the following:

1.- All the values are the same for constraints 1 and 3.

2.- The smaller value of "a_1" occurs in constraint 2, and the largest appears in constraint 4. All the values of "a_2" are the same. The smaller value of "b" occurs in constraint 4, and the largest appears in constraints 1 and 3. The largest value of "h_y" occurs in constraint 2, and the smaller appears in constraints 1, 3 and 4.

3.- The minimum area "A_{min}" is presented in case VI for constraints 1 and 3, and the largest appears in case XIV for constraint 4.

The results of the table 7 show the following:

1.- The smaller value of "a_1" occurs in constraint 3, and the largest appears in constraint 4. All the values of "a_2" are the same. The largest value of "b" occurs in constraint 3, and the smaller appears in constraint 1, 2 and 4. The largest value of "h_y" occurs in constraint 4, and the smaller appears in constraint 4.

2.- The minimum area "A_{min}" is presented in case XI for constraint 3, and the largest appears in case VI for constraint 2.

3.- The constraint 3 shows a rectangular combined footing.

The results of the table 8 show the following:

1.- All the values are the same for constraints 1 and 3, and for constraints 2 and 4.

2.- The smaller value of "a_1" occurs in constraints 1 and 3, and the largest appears in constraints 2 and 4. All the values of "a_2" are the same. All values of "b" are the same. The largest value of "h_y" occurs in constraints 1 and 3, and the smaller appears in constraints 2 and 4.

3.- The minimum area "A_{min}" is presented in case YIIA for constraints 1 and 3, and the largest appears in case YIIA for constraints 2 and 4.

Figure 6 shows a comparison between the CM (current model) and the NM (new model).

Preprints.org (www.preprints.org) | NOT PEER-REVIEWED | Posted: 24 January 2025 doi:10.20944/preprints202501.1740.v1

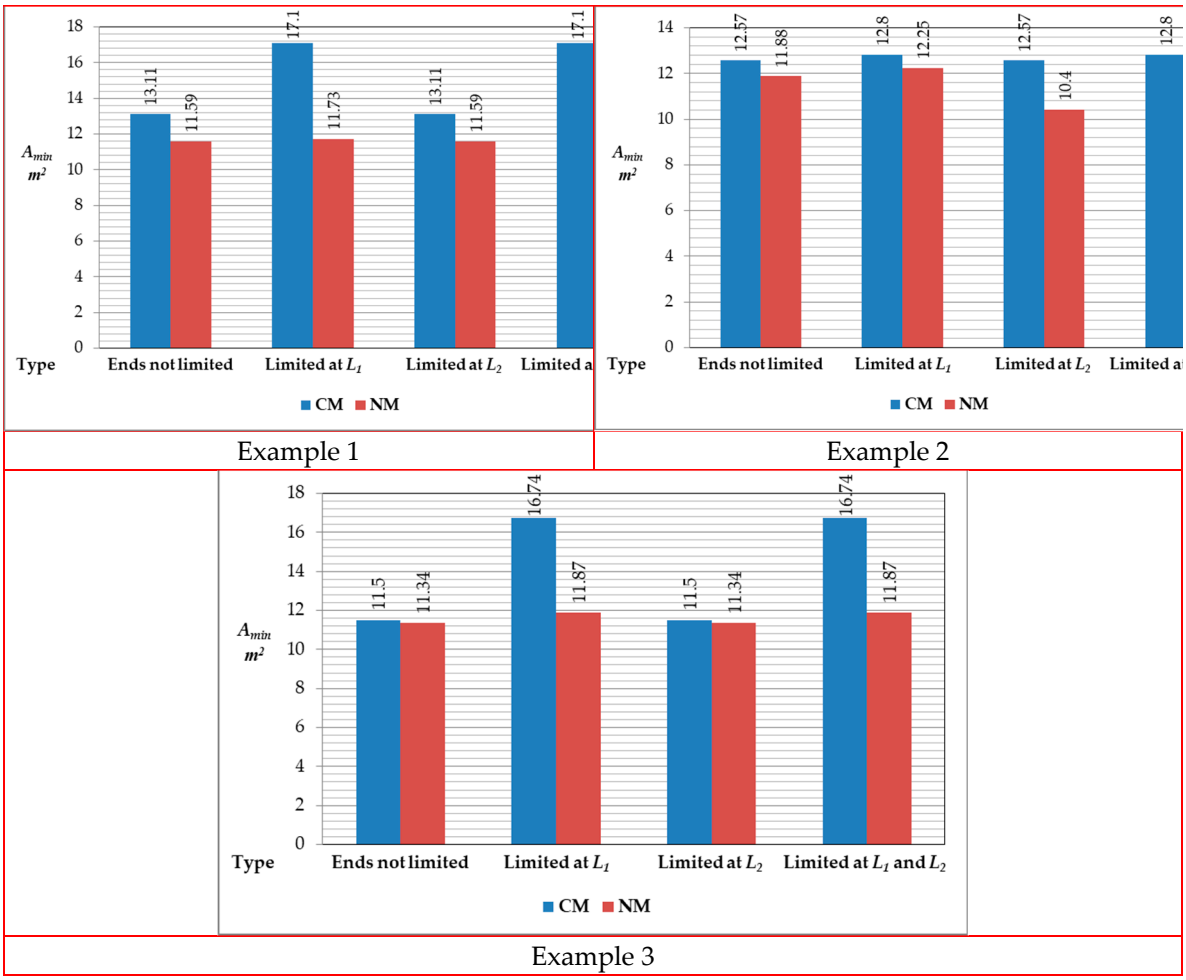

Figure 6. Comparison between the CM and the NM.

In three examples it shows a saving using the NM with respect to the CM. For example 1, largest savings occurs with 31.40% by limiting L_1. For example 2, largest savings occurs with 17.26% by limiting L_2. For example 3, largest savings occurs with 29.09% by limiting L_1, and by limiting L_1 and L_2.

5. Conclusions

The model presented in this document applies only for minimum area of a T-shaped combined footing that supports two columns aligned on a longitudinal axis. The considerations of this work are: the footing is rigid and the soil that supports to the footing is elastic and homogeneous, that comply with the biaxial bending, i.e., the variation of soil pressure is linear.

This paper concludes the following:

1.- Some authors present equations to find the dimensions of the footing and the minimum surface, but the entire surface of the footing works under compression (see Case I for the three examples).

2.- The proposed model presents the minimum surface and the constraint functions for the fifteen possible cases.

3.- The model can be used as a review of the allowable load capacity of the soil, taking into account the objective function "σ_{max}", and the same constraint functions for biaxial bending or uniaxial bending.

4.- The proposed model can be used for rectangular combined footings, simply set $a_1 = a_2$ and $b = h_y$ (see Table 7).

5.- When M_{xT} is zero, the resultant force lies along the X axis (see Table 7).

6.- When M_{yT} is zero, the resultant force lies along the Y axis (see Table 8).

Preprints.org (www.preprints.org) | NOT PEER-REVIEWED | Posted: 24 January 2025 doi:10.20944/preprints202501.1740.v1

7.- The model can be used for the following considerations:

a) Unconstrained sides ($L_1 \geq c_1/2$ and $L_2 \geq c_3/2$)

b) A constrained side in column 1 ($L_1 = c_1/2$ and $L_2 \geq c_3/2$)

c) A constrained side in column 2 ($L_1 \geq c_1/2$ and $L_2 = c_3/2$)

d) Two constrained sides (opposite sides) ($L_1 = c_1/2$ and $L_2 = c_3/2$)

The next investigations can be: 1) Minimum area for corner combined footings assuming that the contact area with the ground woks partially under compression. 2) Minimum area for strap combined footings assuming that the contact area with the ground woks partially under compression.

Author Contributions: E.R.D.-G. contributed to the verification of the model, the written review and the discussion of results. A.L.-R. contributed to the original idea of the article, the mathematical development of the new model and coordinated the work in general. G.S.-H. contributed to the verification of the new model and the programming of the MAPLE 15 software. V.M.M.-L. contributed to the elaboration of the Bibliographic review, the elaboration of the figures and tables. A.E.L.-G. contributed to the application of the proposed model (examples).

Funding: The research was funded by the Universidad Autónoma de Coahuila and Universidad Veracruzana, Mexico.

Data Availability Statement: No new data were created or analyzed in this study. Data sharing is not applicable to this article.

Acknowledgments: The research described in this work was developed at the Universidad Autónoma de Coahuila and Universidad Veracruzana, Mexico.

Conflicts of Interest: The authors declare no conflict of interest.

References

1. Bowles, J.E. *Foundation analysis and design*; McGraw-Hill, New York, USA, 2001.
2. Shahin, M.A.; Cheung, E.M. Stochastic design charts for bearing capacity of strip footings. *Geomech. Eng.* **2011**, *3*, 153-167. https://doi.org/10.12989/gae.2011.3.2.153
3. Dixit, M.S.; Patil K.A. Experimental estimate of Nγ values and corresponding settlements for square footings on finite layer of sand. *Geomech. Eng.* **2013**, *5*, 363-377. https://doi.org/10.12989/gae.2013.5.4.363
4. ErzÍn, Y.; Gul, T.O. The use of neural networks for the prediction of the settlement of pad footings on cohesionless soils based on standard penetration test. *Geomech. Eng.* **2013**, *5*, 541-564. https://doi.org/10.12989/gae.2013.5.6.541
5. Colmenares, J.E.; Kang, S-R.; Shin, Y-J.; Shin, J-H. Ultimate bearing capacity of conical shell foundations. *Struct. Eng. Mech.* **2014**, *52*, 507-523. https://doi.org/10.12989/sem.2014.52.3.507
6. Cure, E.; Sadoglu, E.; Turker, E.; Uzuner, B.A. Decrease trends of ultimate loads of eccentrically loaded model strip footings close to a slope. *Geomech. Eng.* **2014**, *6*, 469-485. https://doi.org/10.12989/gae.2014.6.5.469
7. Fattah, M.Y.; Yousif, M.A.; Al-Tameemi, S.M.K. Effect of pile group geometry on bearing capacity of piled raft foundations", *Struct. Eng. Mech.* **2015**, *54*, 829-853. https://doi.org/10.12989/sem.2015.54.5.829
8. Uncuoğlu, E. The bearing capacity of square footings on a sand layer overlying clay", *Geomech. Eng*. **2015**, *9*, 287-311. https://doi.org/10.12989/gae.2015.9.3.287
9. Anil, Ö.; Akbaş, S.O.; BabagĪray, S.; Gel, A.C.; Durucan, C. Experimental and finite element analyses of footings of varying shapes on sand", *Geomech. Eng.* **2017**, *12*, 223-238. https://doi.org/10.12989/gae.2017.12.2.223
10. Khatri, V.N.; Debbarma, S.P.; Dutta, R.K.; Mohanty, B. Pressure-settlement behavior of square and rectangular skirted footings resting on sand. *Geomech. Eng.* **2017**, *12*, 689-705. https://doi.org/10.12989/gae.2017.12.4.689
11. Mohebkhah, A. Bearing capacity of strip footings on a stone masonry trench in clay. *Geomech. Eng.* **2017**, *13*, 255-267. https://doi.org/10.12989/gae.2017.13.2.255

Preprints.org (www.preprints.org) | NOT PEER-REVIEWED | Posted: 24 January 2025 doi:10.20944/preprints202501.1740.v1

12. Zhang, W.-X.; Wu, H.; Hwang, H.-J.; Zhang, J.-Y.; Chen, B.; Yi, W.-J. Bearing behavior of reinforced concrete column-isolated footing substructures. *Eng. Struct.* **2019**, 200, 109744. https://doi.org/10.1016/j.engstruct.2019.109744
13. Turedi, Y.; Emirler, B.; Ornek, M.; Yildiz, A. Determination of the bearing capacity of model ring footings: Experimental and numerical investigations. *Geomech. Eng.* **2019**, *18*, 29-39. https://doi.org/10.12989/gae.2019.18.1.029
14. Gnananandarao, T.; Khatri, V.N.; Dutta, R.K. Bearing capacity and settlement prediction of multi-edge skirted footings resting onsand. *Ing. Investig.* **2020**, *40*, 9-21. https://doi.org/10.15446/ing.investig.v40n3.83170
15. Gör, M. Analyzing the bearing capacity of shallow foundations on two-layered soil using two novel cosmology-based optimization techniques. *Smart Struct. Syst.* **2022**, *29*, 513-522. https://doi.org/10.12989/sss.2022.29.3.513
16. Chaabani, W.; Remadna, M.S.; Abu-Farsakh, M. Numerical Modeling of the Ultimate Bearing Capacity of Strip Footings on Reinforced Sand Layer Overlying Clay with Voids. Infrastructures **2023**, *8*, 3. https://doi.org/10.3390/infrastructures8010003
17. Vitone, D.M.A.; Valsangkar, A.J. Stresses from loads over rectangular areas. *J. Geotech. Geoenviron.* **1986**, *112*, 961-964. https://doi.org/10.1061/(ASCE)0733-9410(1986)112:10(961)
18. Michalowski, R.L. Upper-bound load estimates on square and rectangular footings. *Géotechnique*. **2001**, *51*, 787-798. https://doi.org/10.1680/geot.2001.51.9.787
19. Özmen, G. Determination of base stresses in rectangular footings under biaxial bending. *Teknik Dergi Digest*. **2011**, *22*, 1519-1535. http://www.imo.org.tr/resimler/dosya_ekler/7b559795bd3f63b_ek.pdf?dergi=472
20. Aydogdu, I. New Iterative method to Calculate Base Stress of Footings under Biaxial Bending. *IJEAS*. **2016**, *8*, 40-48. https://doi.org/10.24107/ijeas.281460
21. Girgin, K. Simplified formulations for the determination of rotational spring constants in rigid spread footings resting on tensionless soil. *JCEM*. **2017**, *23*, 464-474. https://doi.org/10.3846/13923730.2016.1210218
22. Al-Gahtani, H.J.; Adekunle, S.K. A boundary-type approach for the computation of vertical stresses in soil due to arbitrarily shaped foundations. *World J. Eng*. **2019**, *16*, 419-426. https://doi.org/10.1108/WJE-02-2018-0051
23. Rawat, S.; Mittal, R.K.; Muthukumar, G. Isolated Rectangular Footings under Biaxial Bending: A Critical Appraisal and Simplified Analysis Methodology. *Pract. Period. Struct. Des. Const*. **2020**, *25*. https://doi.org/10.1061/(ASCE)SC.1943-5576.0000471
24. López-Machado, N.A.; Perez, G.; Castro, C.; Perez, J.C.V.; López-Machado, L.J.; Alviar-Malabet, J.D.; Romero-Romero, C.A.; Guerrero-Cuasapaz, D.P.; Montesinos-Machado, V.V. A Structural Design Comparison Between Two Reinforced Concrete Regular 6-Level Buildings using Soil-Structure Interaction in Linear Range. *Ing. Investig.* **2022**, 42, e86819. https://doi.org/10.15446/ing.investig.v42n1.86819
25. Lezgy-Nazargah, M.; Mamazizi, A.; Khosravi, H. Analysis of shallow footings rested on tensionless foundations using a mixed finite element model. *Struct. Eng. Mech.* **2022**, *81*, 379-394. https://doi.org/10.12989/sem.2022.81.3.379
26. Teng, W.C. *Foundation Design*; Prentice-Hall Inc.: New Delhi, India, 1979.
27. Highter, W.H.; Anders, J.C. Dimensioning footings subjected to eccentric loads. *J. Geotech. Geoenviron.* **1985**, *111*, 659-665. https://doi.org/10.1061/(ASCE)0733-9410(1985)111:5(659)
28. Galvis, F.A.; Smith-Pardo, P.J. Axial load biaxial moment interaction (PMM) diagrams for shallow foundations: Design aids, experimental verification, and examples. *Eng. Struct*. **2020**, *213*, 110582. https://doi.org/10.1016/j.engstruct.2020.110582
29. Rodriguez-Gutierrez, J.A.; Aristizabal-Ochoa, J.D. Rigid spread footings resting on soil subjected to axial load and biaxial bending. I: Simplified analytical method. *Int. J. Geomech.* **2013**, *13*, 109-119. https://doi.org/10.1061/(ASCE)GM.1943-5622.0000218
30. Rodriguez-Gutierrez, J.A.; Aristizabal-Ochoa, J.D. Rigid spread footings resting on soil subjected to axial load and biaxial bending. II: Design aids. *Int. J. Geomech.* **2013**, *13*, 120-131. https://doi.org/10.1061/(ASCE)GM.1943-5622.0000210

Preprints.org (www.preprints.org) | NOT PEER-REVIEWED | Posted: 24 January 2025 doi:10.20944/preprints202501.1740.v1

31. Maheshwari, P.; Khatri, S. Influence of inclusion of geosynthetic layer on response of combined footings on stone column reinforced earth beds. *Geomech. Eng.* **2012**, *4*, 263-279. https://doi.org/10.12989/gae.2012.4.4.263
32. Konapure, C.G.; Vivek, B. Analysis of Combined rectangular footing by Winkler's Model and Finite Element Method. *International JEIT*. **2013**, *3*, 128-132. https://www.ijeit.com/Vol%203/Issue%205/IJEIT1412201311_21.pdf
33. Vivek, B.; Arkal, L.S.; Bandgar, R.V.; Kalekhan, F.A.S. Comparative Study on Conventional and Simplified Elastic Analysis of Rectangular Combined Footing. *Int. J. Res. Eng. Technol.*,¿ **2014**, *3*, 422-427. https://ijret.org/volumes/2014v03/i04/IJRET20140304076.pdf
34. Ravi Kumar Reddy, C.; Satish Kumar, M.; Kondala Rao, M.; Gopika, N. Numerical Analysis of Rectangular Combined Footings Resting on Soil for Contact Pressure. *Int. J. Civil Engi. Technol*. **2018**, *9*, 1425-1431. http://iaeme.com/Home/issue/IJCIET?Volume=9&Issue=9
35. Kashani, A.R.; Camp, C.V.; Akhani, M.; Ebrahimi, S. Optimum design of combined footings using swarm intelligence-based algorithms. *Adv. Eng. Soft*. **2022**, *169*, 103140. https://doi.org/10.1016/j.advengsoft.2022.103140
36. Al-Douri, E.M.F. Optimum design of trapezoidal combined footings. *Tikrit J. Eng. Sci*. **2007**, 14, 85–115. https://doi.org/10.25130/tjes.14.1.05
37. Luévanos-Rojas, A. Optimization for trapezoidal combined footings: Optimal design. Adv. *Concrete Constr., Int. J*. **2023**, *16*, 21-34. https://doi.org/10.12989/acc.2023.16.1.021
38. Luévanos-Rojas, A.; López-Chavarría, S.; Medina-Elizondo, M. A new model for T-shaped combined footings Part I: Optimal dimensioning. *Geomech. Eng*. **2018**, *14*, 51-60. https://doi.org/10.12989/gae.2018.14.1.051
39. Luévanos-Rojas, A.; López-Chavarría, S.; Medina-Elizondo, M. A new model for T-shaped combined footings Part II: Mathematical model for design. *Geomech. Eng*. **2018**, *14*, 61-69. http://dx.doi.org/10.12989/gae.2018.14.1.061
40. Moreno-Landeros, V.M.; Luévanos-Rojas, A.; SantiagoHurtado, G.; López-León, L.D.; Olguin-Coca, F.J.; López-León, A.L.; Landa-Gómez, A.E. Optimal Cost Design of RC T-Shaped Combined Footings. *Buildings* 2024, 14, 3688. https://doi.org/10.3390/buildings14113688
41. Aishwarya, K.M.; Balaji, N.C. Analysis and design of eccentrically loaded corner combined footing for rectangular columns. International Conference on Advances in Sustainable Construction Materials, Guntur, India, 18-19 March **2022**. https://doi.org/10.1063/5.0144289
42. Luévanos-Rojas, A.; Santiago-Hurtado, G.; Moreno-Landeros, V.M.; Olguin-Coca, F.J.; López-León, L.D.; Diaz-Gurrola, E.R. Mathematical Modeling of the Optimal Cost for the Design of Strap Combined Footings. *Mathematics* 2024, 12, 294. https://doi.org/10.3390/math12020294

Disclaimer/Publisher's Note: The statements, opinions and data contained in all publications are solely those of the individual author(s) and contributor(s) and not of MDPI and/or the editor(s). MDPI and/or the editor(s) disclaim responsibility for any injury to people or property resulting from any ideas, methods, instructions or products referred to in the content.